

Journal Pre-proofs

Discovery of novel pyrazolo[3,4-b]pyridine scaffold-based derivatives as potential PIM-1 kinase inhibitors in breast cancer MCF-7 cells

Mohamed S. Nafie, Atef M. Amer, Anaiat K. Mohamed, Eman S. Tantawy

PII: S0968-0896(20)30658-1
DOI: <https://doi.org/10.1016/j.bmc.2020.115828>
Reference: BMC 115828

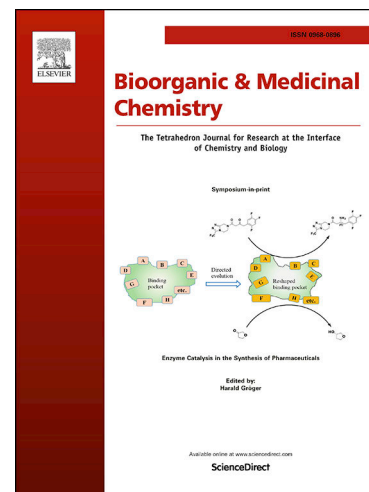
To appear in: *Bioorganic & Medicinal Chemistry*

Received Date: 10 August 2020
Revised Date: 15 October 2020
Accepted Date: 22 October 2020

Please cite this article as: M.S. Nafie, A.M. Amer, A.K. Mohamed, E.S. Tantawy, Discovery of novel pyrazolo[3,4-b]pyridine scaffold-based derivatives as potential PIM-1 kinase inhibitors in breast cancer MCF-7 cells, *Bioorganic & Medicinal Chemistry* (2020), doi: <https://doi.org/10.1016/j.bmc.2020.115828>

This is a PDF file of an article that has undergone enhancements after acceptance, such as the addition of a cover page and metadata, and formatting for readability, but it is not yet the definitive version of record. This version will undergo additional copyediting, typesetting and review before it is published in its final form, but we are providing this version to give early visibility of the article. Please note that, during the production process, errors may be discovered which could affect the content, and all legal disclaimers that apply to the journal pertain.

© 2020 Published by Elsevier Ltd.



Discovery of novel pyrazolo[3,4-*b*]pyridine scaffold-based derivatives as potential PIM-1 kinase inhibitors in breast cancer MCF-7 cells

Mohamed S. Nafie ^{a*}, Atef M. Amer ^b, Anaiat K. Mohamed ^b, Eman S. Tantawy ^b

^a Chemistry Department, Faculty of Science, Suez Canal University, Ismailia (41522), Egypt, <https://orcid.org/0000-0003-4454-6390>

^b Department of Chemistry, Faculty of Science, Zagazig University, Egypt.

Abstract:

Pim-1 kinase targeted recently has proved an essential goal of breast cancer therapy. We report the design, synthesis with full characterization analysis of pyrazolo[3,4-*b*]pyridine scaffold-based derivatives targeting Pim-1 kinase as anti-breast cancer agents. All the newly synthesized compounds were screened for their *in vitro* cytotoxic activity against two breast cancer cell lines MCF-7 and MDA-MB-231, and non-cancerous MCF-10A cells. Four derivatives notably, **17** and **19** exhibited a remarkable cytotoxic activity with IC₅₀ values 5.98 and 5.61 μM against MCF-7 (ERα-dependent) cells in a selective way, as they weren't active against MDA-MB-231 (non-ERα-dependent) and safe against MCF-10A. The most active compounds through *in vitro* screening were subjected to PIM-1 kinase to elucidate the Pim-1 kinase inhibitory activity as the mechanistic mode of action. Among the tested derivatives, Compounds **17** and **19** showed the highest inhibitory activity with IC₅₀ values 43 and 26 nM, respectively, compared to the 5-FU with IC₅₀ value 17 nM. Moreover, apoptotic investigation through flow cytometry and gene expression analysis of the apoptosis-related genes for the most active compound **19** against MCF-7. It was found that compound **19** induced apoptotic MCF-7 cell death by cell cycle arrest at G2/M phase and by elevation the expression of pro-apoptotic genes and inhibition of anti-apoptotic genes expression. Finally, the PIM-1 inhibition activities for compounds **17** and **19** were in accordance with the molecular docking study that revealed good interaction with the Pim-1 kinase active site.

Keywords: Apoptosis, Breast cancer, Docking, PIM-1 kinase, Pyrazolo-pyridines.

*Corresponding author: Mohamed_nafie@science.suez.edu.eg (Mohamed S. Nafie), Chemistry Department, Faculty of Science, Suez Canal University, Ismailia (41522)

 <https://orcid.org/0000-0003-4454-6390>

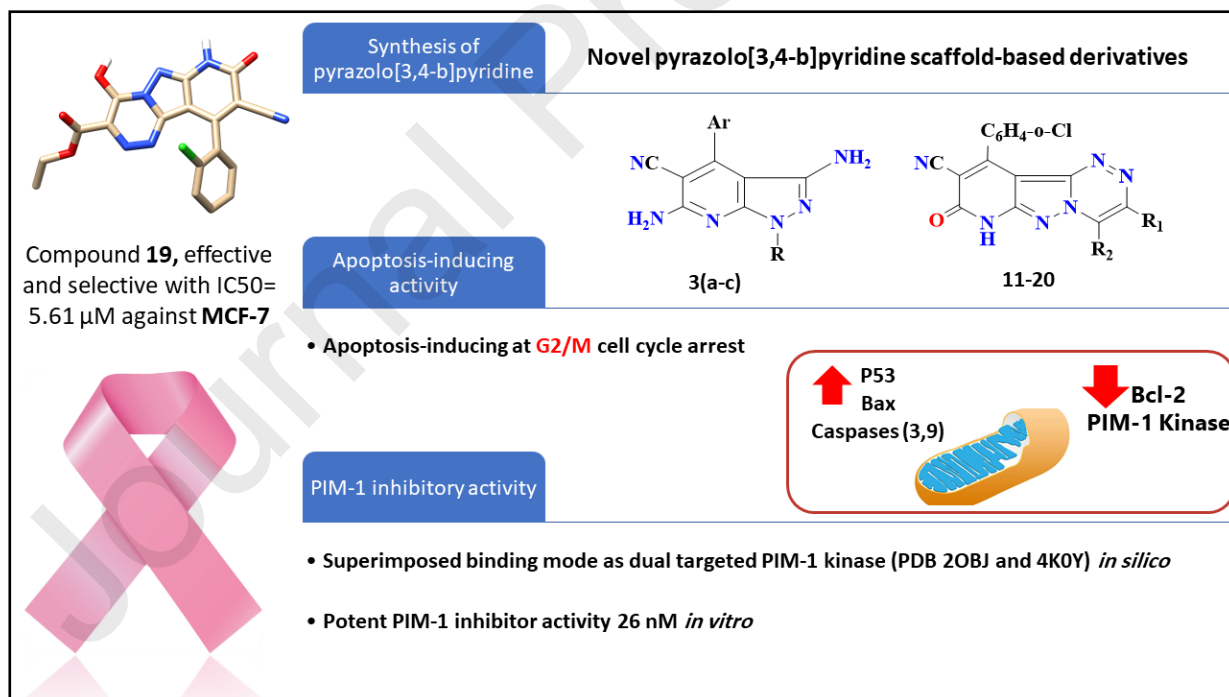
List of abbreviations

Proto-oncogene serine/threonine (PIM-1) kinase; half minimal inhibitor concentration (IC_{50}); 5-fluorouracil (5-FU); cycle threshold (Ct); melting point (m.p.); 3-(4,5-dimethylthiazol-2-yl)-2,5-diphenyltetrazolium bromide (MTT); human breast cancer cell lines (MCF-7, MDA-MB-231); normal breast cell line (MCF-10A); estrogen dependent (ER), millilitre/microlitre (mL/ μ l) standard error of mean (SEM), propidium iodide (PI), cell cycle phases (Pre G1, G0/G1, S, G2/M).

Highlights

- Novel pyrazolo[3,4-b]pyridine scaffold-based derivatives were synthesized and characterized.
- Both Compound **17** and **19** were found to be potent and selective against MCF-7 cells through apoptosis-inducing activity.
- Both compounds **17** and **19** were good inhibitors for PIM-1 kinase in both enzymatic, RT-PCR, and *in silico* assays.

Graphical abstract



1. Introduction

Breast cancer has been the most prevalent cancer in women among the different types of malignant tumors reported to date. It represents the second most important cause of death in women ¹. Despite the significant efforts devoted to fight against various types of cancer, yet this disease is still one of the biggest global concerns. Therefore, the discovery of new anti-cancer drugs with potent molecular targets, among which PIM-1 as a novel potential target gene for breast cancer therapy ², is always in demand.

PIM kinases, including “Pim1, Pim2, and Pim3” have grown as attractive pharmacological objectives in cancer therapy due to their role in the growth, cellular survival, and tumor genesis of cells ^{3,4}. Pim-1 kinase is a serine/threonine kinase that regulates multiple cellular functions such as cell cycle, cell survival, so Pim-1 kinase is linked to many cancer types ⁵. Pim-1 kinases have the luxury to have a unique structure on their binding site and to design small micro-cellular with high selectiveness inhibitors of PIM-1 kinase ⁶. Moreover, multiple cell functions, such as survival, apoptosis, differentiation, and the proliferation of numerous cancers, including the breast, are involved ^{7,8}. There is, therefore, an essential strategy for treating breast cancer as PIM-1 kinase inhibitors. The targeting of Pim-1 kinases via the production of selective small molecular inhibitors, therefore, constitutes a promising strategy for suppressing both apoptosis induction and tumor proliferation ⁹⁻¹¹.

Most 1H pyrazol[3,4-b]pyridine polysubstituted derivatives had been synthesized as potentially biologically active compounds and had a multitude of pharmacological characteristics, in particular, anti-cancer activity ¹²⁻¹⁴. 1H-pyrazolo[3,4-b]pyridine is one of the promising heterocycle classes with highly tolerated and anti-tumor activities in humans. Moreover, fused heterocyclic containing pyrazolopyridine systems have been reported to have anti-tumor activity ¹⁵⁻¹⁹.

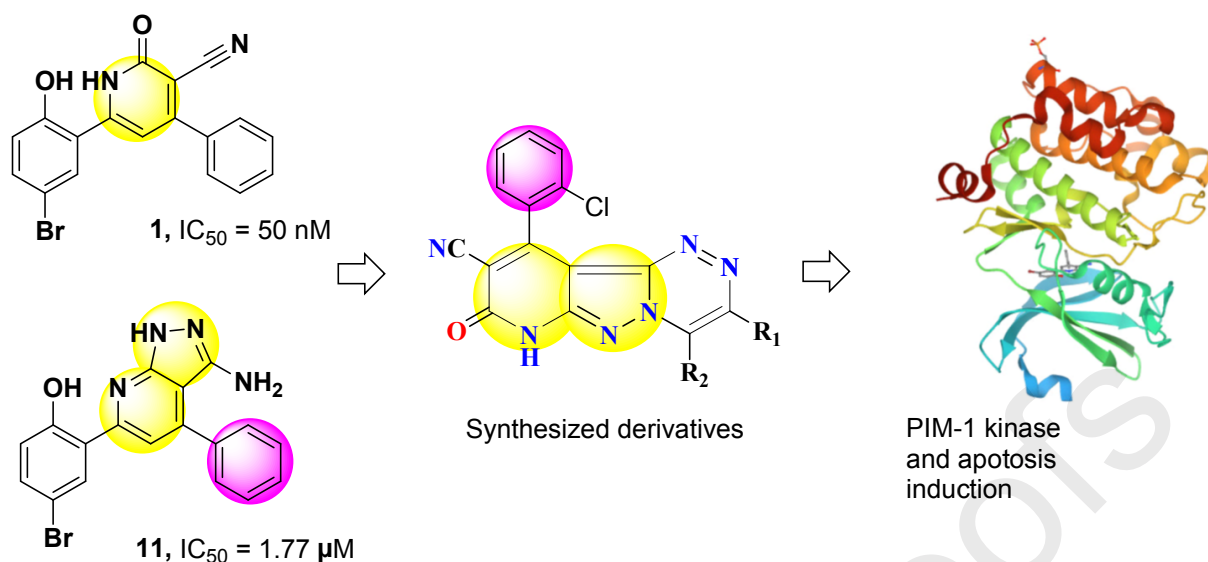


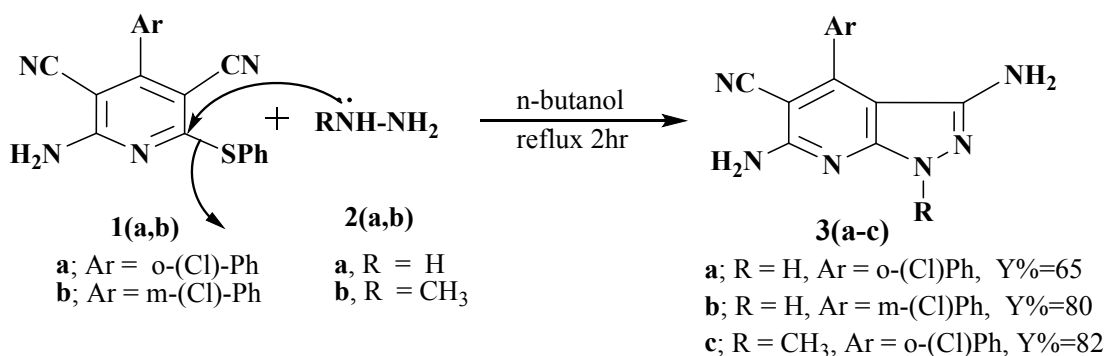
Fig. (1): Rational drug design for the synthesis of the tested pyrazolo[3,4-b]pyridine scaffold-based derivatives

According to Cheney et al. 2007²⁰, a new set of highly active substituted pyridone (Compound **1**, $IC_{50} = 50 \text{ nM}$) and substituted pyrazolo pyridine (Compound **11**, $IC_{50} = 1.77 \mu\text{M}$), as Pim-1 kinase inhibitors were described. The program is aimed towards the synthesis of heterocyclic fused nitrogen compounds. It extends efforts to develop convenient synthetic approaches to synthesize fused pyrazolopyridine derivatives with a wide range of biological activities to be expected. This research aims to investigate the main structural requirements for Pim-1 kinase inhibition using the modeling mentioned above combination Fig. (1) to develop novel pyrazol[3,4-b]pyridine derivatives as Pim-1 kinase inhibitors and to be screened for their cytotoxicity against two types of breast cancer cell lines, investigating their apoptotic cell death activity. Our rationalization for synthesis is in accordance with El-Gohary et al. 2018, 2019²¹⁻²³, who synthesized and tested a series of pyrazolo[3,4-b]pyridine derivatives as potent anti-cancer agents.

2. Results and Discussion

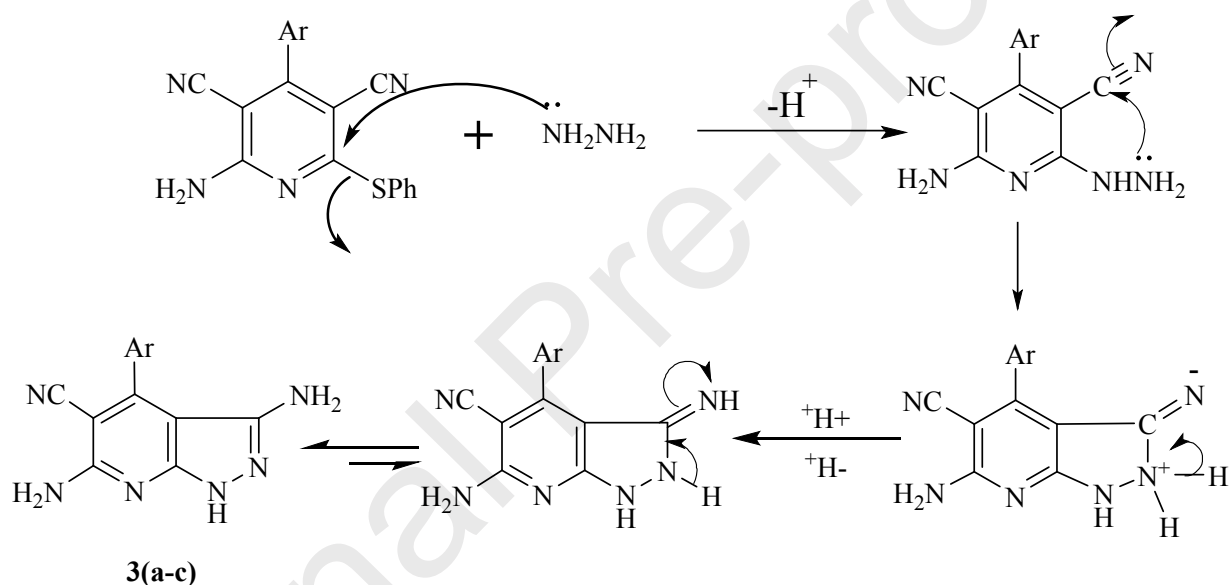
2.1. Chemistry and structure elucidation

In the present work, we describe a simple method for synthesis of 3,6-diamino-4-aryl-pyrazolo[3,4-*b*]pyridine-5-carbonitrile derivatives **3a-c** by the reaction of 3,6-diaminopyrazolo[3,4-*b*]pyridine-3,5-dicarbonitrile **1a,b** with hydrazine hydrate and/or methyl hydrazine afforded **3a-c** in good yield Scheme (1), Very close analogues were previously reported^{24,25}.

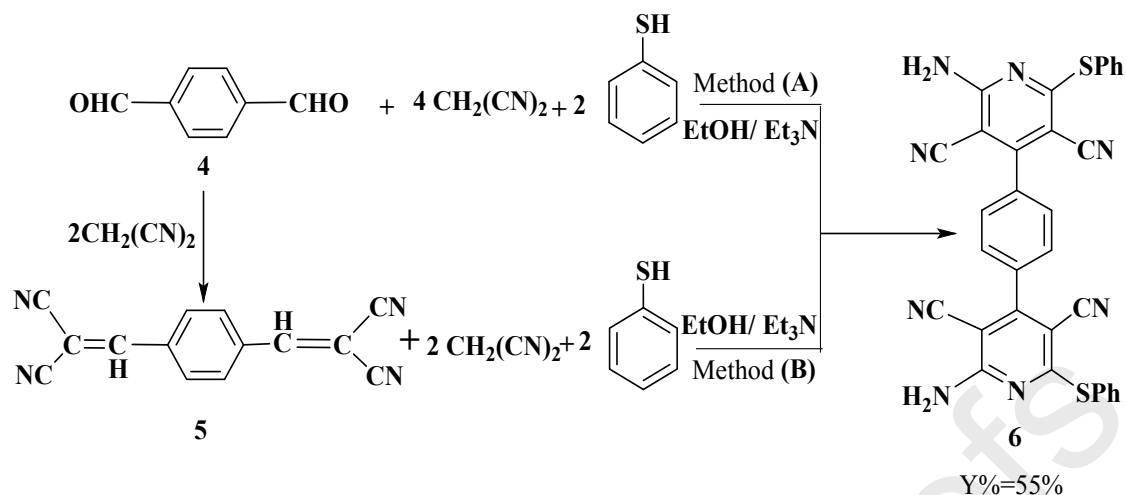


Scheme (1): Synthesis of 3,6-diamino-4-aryl-pyrazolo[3,4-b]pyridine-5-carbonitrile derivatives **3(a-c)**

The reaction took place via thiophenol elimination and cyclization according to the following mechanism



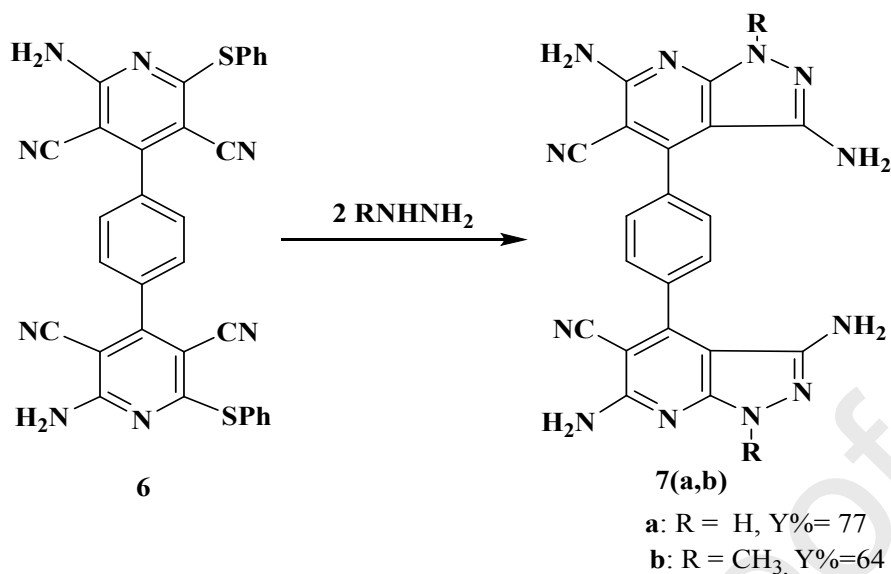
Similarly, treatment of terephthalaldehyde **4** with four equivalent moles of malononitrile and two moles from thiophenol in ethanol and triethyl amines under refluxing condition afforded compound **6** in good yield (Method A). Also, compound **6** afforded by the reaction of arylidene- malononitrile **5** with two moles of malononitrile and two moles of thiophenol in ethanol and triethylamine under refluxing condition (Method B) as shown in scheme (2) [26]



Scheme (2): Synthesis of compound **6** using two methods (A&B)

The chemical structure of 4,4'-(1,4-phenylene)bis(2-amino-6-(phenylthio)pyridine-3,5-dicarbonitrile) **6** was confirmed by elemental analysis and spectral data. The IR spectrum of **6** showed broad bands at 3451, 3329 and 3217 cm^{-1} characteristic to two NH_2 groups, double bands at 2209 cm^{-1} due to four cyano groups, and at 1621 cm^{-1} due to $\text{C}=\text{N}$ group. The $^1\text{H-NMR}$ spectrum of **6** in CDCl_3 exhibited two bands at δ 5.47 due to 2 NH_2 groups and multiplet signals centered 7.10-7.68 due to Ar-H. Also, the $^1\text{H-NMR}$ spectrum of **6** in $\text{DMSO-}d_6$ showed singlet signals at δ 6.00, 6.82 characteristic for NH_2 groups, and 7.42-7.85 due to Ar-H. The mass spectrum of compound **6** exhibited a strong molecular ion peak at m/e 576 for $[\text{M}^+-2]$, the base peak at 169 (100%), and aromatic fragmentation.

The reaction of 4,4'-(1,4-phenylene)bis(2-amino-6-(phenylthio)pyridine-3,5-dicarbonitrile) **6** with hydrazine hydrate or methyl hydrazine gives 4,4'-(1,4-phenylene)bis(3,6-diamino-1*H*-pyrazolo[3,4-*b*]pyridine-5-carbonitrile) **7a** and 4,4'-(1,4-phenylene)bis(3,6-diamino-1-methyl-1*H*-pyrazolo[3,4-*b*]pyridine-5-carbonitrile) **7b** respectively via two moles from thiophenol elimination and cyclization Scheme (3).

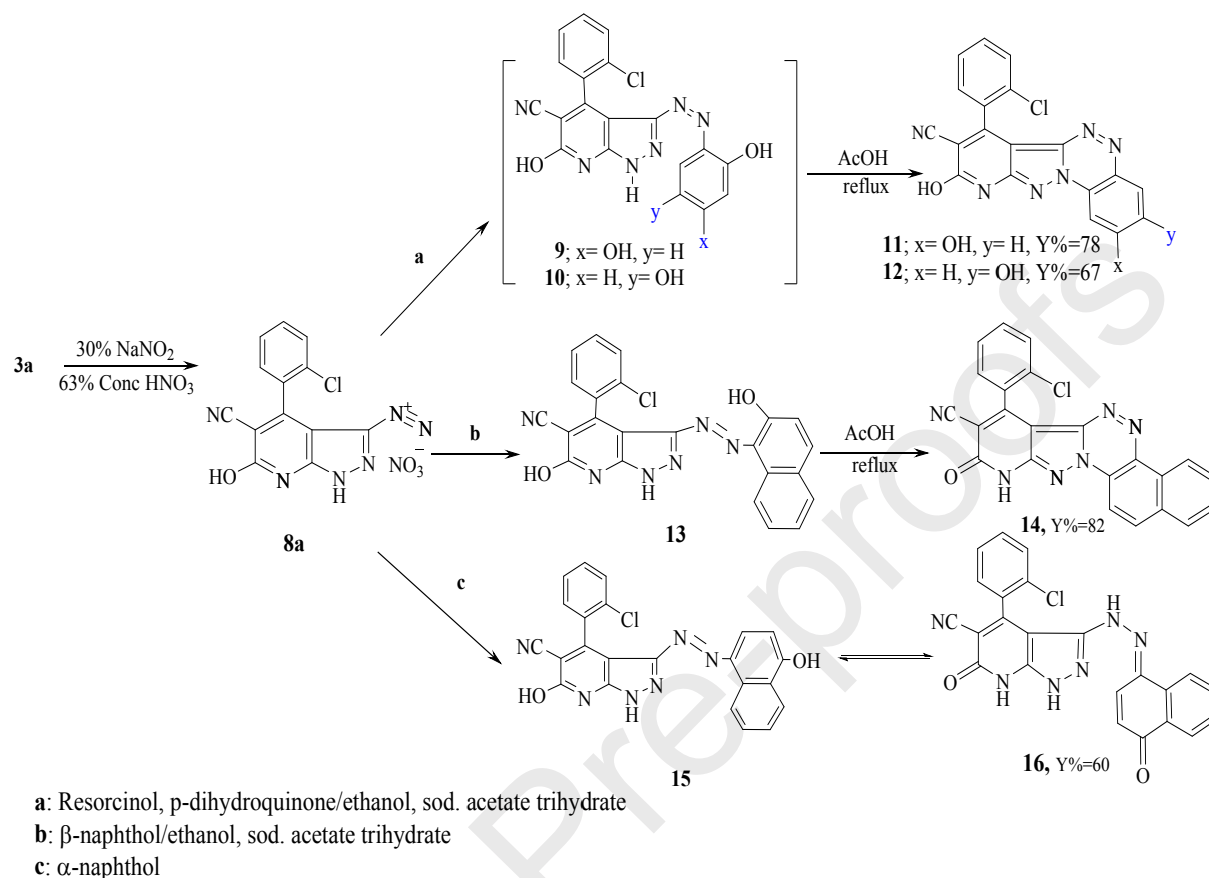


Scheme (3): Synthesis of 7(a,b)

The IR spectra of **7a** showed absorption bands at 3460, 3302, and 3215 cm^{-1} characteristics to four amino groups, 2205 cm^{-1} due to two cyano groups, and 1633 cm^{-1} due to C=N bonds. The $^1\text{H-NMR}$ spectrum of **7a** showed broad signals at δ 4.26 for 2NH₂ of pyrazole, doublet signals at δ 6.85-6.95 for 2NH₂ pyridine, multiplet signals at δ 7.33-7.78 for Ar-H and broad signals at δ 11.65, 11.85 for 2NH pyrazole. The mass spectrum of compound **7a** showed a molecular ion peak at 421 (M^+-1) and a base peak at 112 (100%). The $^1\text{H-NMR}$ spectrum of **7b** showed singlet signals at δ 3.62 characteristic to 2CH₃, broad signals at δ 4.60 for 2NH₂ pyrazole, singlet signals at δ 6.90 characteristic to 2NH₂ of pyridine.

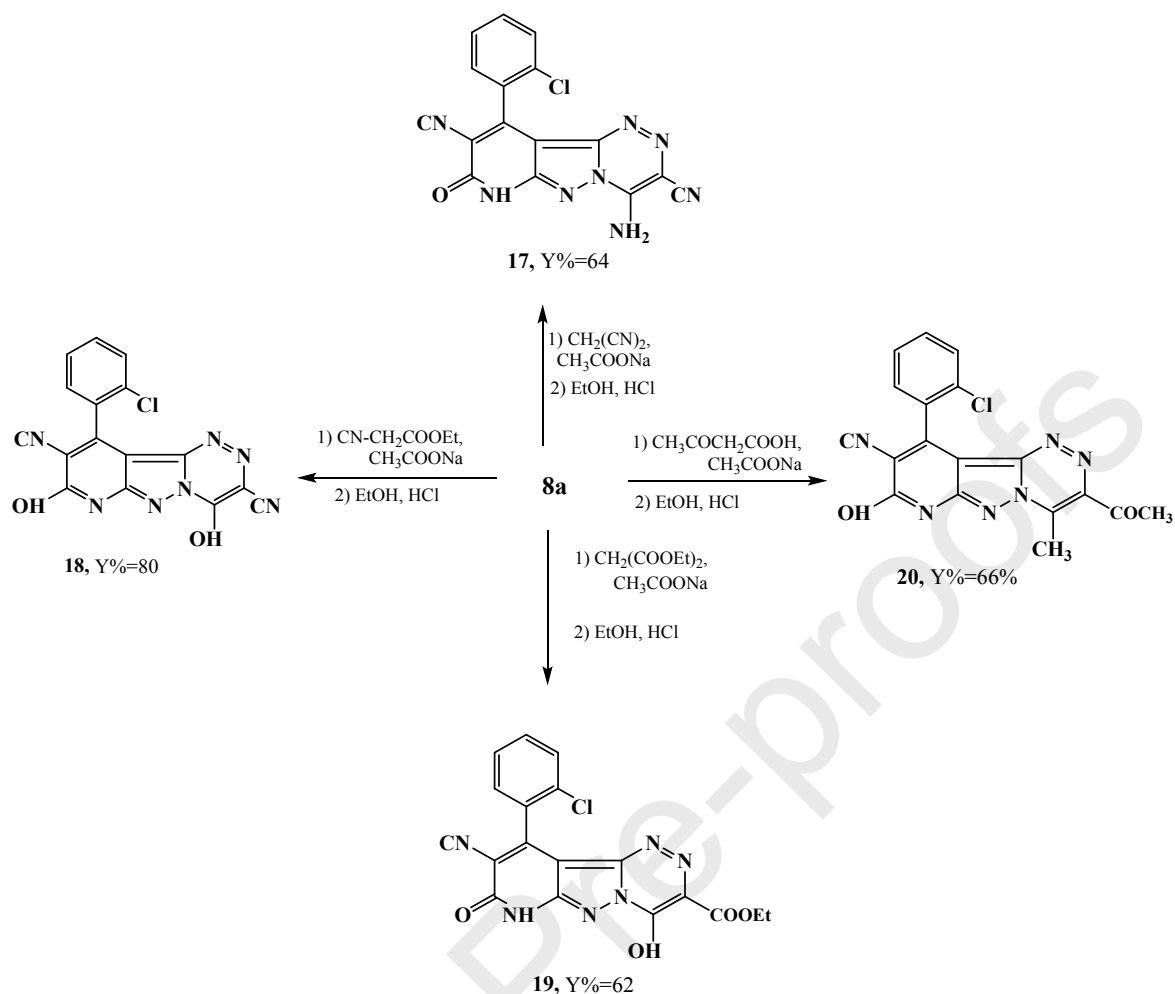
From our present work, the 3-amino group in 4-(2-chlorophenyl)-3,6-diaminopyrazolo[3,4-*b*]pyridine-5-carbonitrile **3a** behaves as atypical aromatic amine, while the 6-amino group is converted into a hydroxyl group (or rather the pyridine tautomer) under diazotization condition. Treatment of **3a** with NaNO₂ and Conc HNO₃ afforded the diazonium salt **8a**. The diazonium salt **8a** couples with resorcinol, *p*-dihydroquinone and β -naphthol in ethanolic solution in the presence of sodium acetate trihydrate to give the corresponding azo compounds and this can be subsequently converted into **11**, **12** and **14** respectively on treatment with acetic acid at reflux temperature Scheme (4). Furthermore, the coupling of the diazonium salt **8a** with α -naphthol to give corresponding 4-(2-chlorophenyl)-6-oxo-3-(2-(4-oxonaphthalen-1(4*H*)-ylidene)-6,7-dihydro-1*H*-pyrazolo[3,4-*b*]pyridine-5-carbonitrile **16**. The $^1\text{H-NMR}$ spectra of **11**, **12** and **14** give singlet signals at δ 12.30, 13.76, and 13.50 ppm due to the pyridine NH, which disappear by deuteration with D₂O. The $^1\text{H-NMR}$ of **16** exhibited

multiplet signals centered at 7.10-8.35 characteristic for aromatic protons, broad signals at δ 10.0 for OH and δ 12.80 for NH of pyridone.



Scheme (4): Diazotisation of 3,6-diamino-4-(2-chlorophenyl)-1H-pyrazolo[3,4-b]pyridine (**3a**) and coupling with active hydrogen reagent

The reaction of diazotised of 3,6-diamino-4-(2-chlorophenyl)-1H-pyrazolo[3,4-b]pyridine-5-carbonitrile **8a** with appropriate active hydrogen reagents, namely malononitrile, ethyl cyanoacetate, diethylmalonate and acetyl acetone were carried out in the presence of sodium acetate to give the corresponding cyclic products. The open derivatives can be cyclized into pyrido[3,2-c]-1,2,4-triazine derivatives **17-20** respectively Scheme (5) when heated in ethanolic solution in the presence of mineral acid (1 mL, HCl)

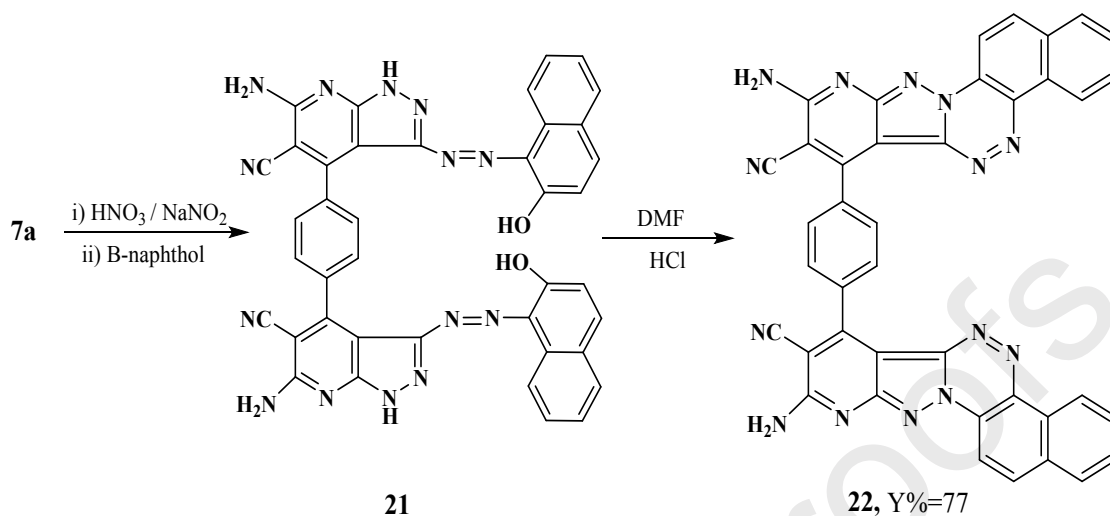


Scheme (5): Synthesis of compounds (**17-19**) by reaction of **8a** with appropriate active hydrogen reagents

The U.V spectrum of **17** in DMF showed λ_{max} at 482, 460, 424, 386, and 344 nm. The IR spectrum of **17** showed absorption bands at 3474 cm^{-1} characteristic to OH, 3320 cm^{-1} for NH₂, 2231 cm^{-1} for cyano group, 1662 cm^{-1} (C=O pyridone). The ¹H-NMR spectrum of **17** showed broad signals at 9.59 for NH₂ and 13.24 for NH. The ¹H-NMR spectrum of **18** in CDCl₃ showed singlet signals at δ 5.78 for two OH groups. The IR spectrum of **19** showed absorption bands at 3454 cm^{-1} for OH, 3312 cm^{-1} for NH, 2924 cm^{-1} (C-H aliphatic bond), 2223 cm^{-1} for cyano group, 2138 cm^{-1} (conjugated cyano group), 1710 cm^{-1} (C=O ester). The ¹H-NMR spectrum of **20** showed a singlet signal at δ 2.04 for CH₃, singlet signal at δ 2.89 for COCH₃ and broad signal at δ 5.58 for OH.

The final part of our work describes the coupling of compound **7a** with two moles of β -naphthol. The coupling was done in the presence of ethanol and sodium acetate to give the cyclic compound **21**, when heated alone as well as in N,N-dimethylformamide solution in the

presence of mineral acid (1 mL, HCl) to give the cyclized compound **22** as shown as Scheme (6).



Scheme (6): Synthesis of compounds **21,22**

The $^1\text{H-NMR}$ spectrum of **22** showed a broad signal at δ 6.60 for 2NH_2 and multiplet signals at δ 7.00-9.00 for Ar-H . The mass spectrum of compound **22** showed molecular ion peak at m/e 692 ($\text{M}^+ - 2$, 16%), 346, 300, 297, 234, 174, 130 and 88.

2.2. Biological evaluation

2.2.1. Cytotoxic activity

Using the MTT assay, all synthesized derivatives were subjected to cytotoxic screening against two breast cancer cell lines one is estrogen-dependent ($\text{ER}\alpha$) and the other is non-estrogen dependent (Non- $\text{ER}\alpha$) to test their activity and selectivity against the tested breast cancer cells. Additionally, they were tested against normal breast cells (MCF-10A) to test their safety (non-toxic activity). Using the same serial dilutions of the tested compounds against the percentage of cell survival, IC_{50} values were calculated as seen in Table (1). The tested compounds, especially **11, 12, 16, 17 and 19** exhibited remarkable cytotoxic activity against MCF-7 with IC_{50} values lower than 10, in a selective way as they aren't active against the MDA-MB-231 and MCF-10A, so these findings showed the activity, selectivity, and safety of these derivatives as anti-breast cancer cells proliferation. Compounds **18, 20, 6, 7a and 22** showed moderate activity against MCF-7 with IC_{50} values higher than 10, with moderate to low activity against MDA-MB-231 except for compound **6**, which exhibited good cytotoxic and selective activity against MDA-MB-231. While, other compounds weren't active against both cell lines. The results of the tested derivatives are in accordance with similar derivatives of cyanopyridine derivatives that were

designed as PIM-1 kinase for a potent anti-proliferative activity against MCF-7 cell line, and they were further tested for their apoptosis-inducing activity ²⁶.

Table (1): Cytotoxic activity of the tested derivatives against two breast cancer cell lines; MCF-7 (ER-dependent), MDA-MB-231 (Non-ER-dependent), and normal breast cells (MCF-10A) using MTT assay.

| Compounds | Breast cancer cell line | | Normal breast cell line |
|-------------|---|------------------|---|
| | IC ₅₀ ^{##} (μ M) | | IC ₅₀ ^{##} (μ M) |
| | MCF-7 | MDA-MB-231 | MCF-10A |
| 3a | 36.6 \pm 0.74 | ND | 20.56 \pm 0.93 |
| 3b | \geq 50 | ND | ND |
| 3c | ND | ND | 53.7 \pm 1.25 |
| 6 | 16.76 \pm 0.87 | ND | 48.7 \pm 1.24 |
| 7a | 17.87 \pm 0.88 | 35.7 \pm 0.07 | 43.6 \pm 1.02 |
| 7b | \geq 50 | ND | \geq 50 |
| 11 | 9.12 \pm 0.24 | 39.5 \pm 0.08 | \geq 50 |
| 12 | 10.02 \pm 0.65 | 24.7 \pm 0.87 | \geq 50 |
| 14 | \geq 50 | 9.76 \pm 0.86 | ND |
| 16 | 8.71 \pm 0.05 | \geq 50 | \geq 50 |
| 17 | 6.98 \pm 0.09 | \geq 50 | \geq 50 |
| 18 | 27.5 \pm 0.24 | 10.6 \pm 0.59 | ND |
| 19 | 5.61 \pm 0.15 | 38.7 \pm 1.03 | 46.8 \pm 1.07 |
| 20 | 14.8 \pm 0.15 | 20.76 \pm 0.29 | ND |
| 22 | 11.43 \pm 0.78 | 43.7 \pm 1.06 | ND |
| 5-FU | 5.8 \pm 0.34 | 15.74 \pm 0.65 | 39.7 \pm 1.05 |

*Values are expressed as Mean \pm SEM of three independent values, **ND** is Not Determined

[#]IC₅₀ values are calculated by using GraphPad prism 7 software; non-linear regression curve fit of sigmoidal dose-response inhibition

2.2. 2. PIM-1 kinase inhibition

PIM kinase has been a primary clinical target to establish new cancer therapies. A search for the mechanistic mode of action for the most active compounds against MCF-7, we screened their activity using human proto-oncogene serine/threonine-protein kinase PIM-1 ELISA kit. As seen

in Table (2), the results exhibited good PIM-1 kinase inhibitory activity appearing from comparing the IC_{50} values. Among the tested derivatives, Compounds **17** and **19** showed the highest inhibitory activity with IC_{50} values 26 and 43 nM, respectively, compared to the Staurosporin with IC_{50} value 17 nM. Moreover, compounds **11** and **16** exhibited moderate inhibitory activity with IC_{50} values 87 and 95 nM, respectively. While compound **12** showed weak inhibitory activity with IC_{50} 112 nM.

Table (2): PIM-1 kinase inhibitory activities of the most active compounds.

| Compounds | $IC_{50} \pm SEM^*$ (nM) |
|--------------------------------------|--------------------------|
| 17 | 43 ± 1.02 |
| 19 | 26 ± 0.98 |
| 11 | 87 ± 1.76 |
| 12 | 112 ± 1.76 |
| 16 | 95 ± 1.25 |
| Staurosporin (reference drug) | 17 |

*Values are expressed as Mean \pm SEM of 3 independent trials

Pyrazolo[3,4-b]pyridine may be found to have elements of compounds pyrrolo[2,3-b]pyridine and indazole components, and therefore, they can use multi-binding modes to interact with kinases²⁷. Following Abdelaziz et al.²⁸, who designed and synthesized series of pyridine and thieno[2,3-b]pyridine derivatives as anti-cancer PIM-1 kinase inhibitors with potent IC_{50} = 0.019 μ M.

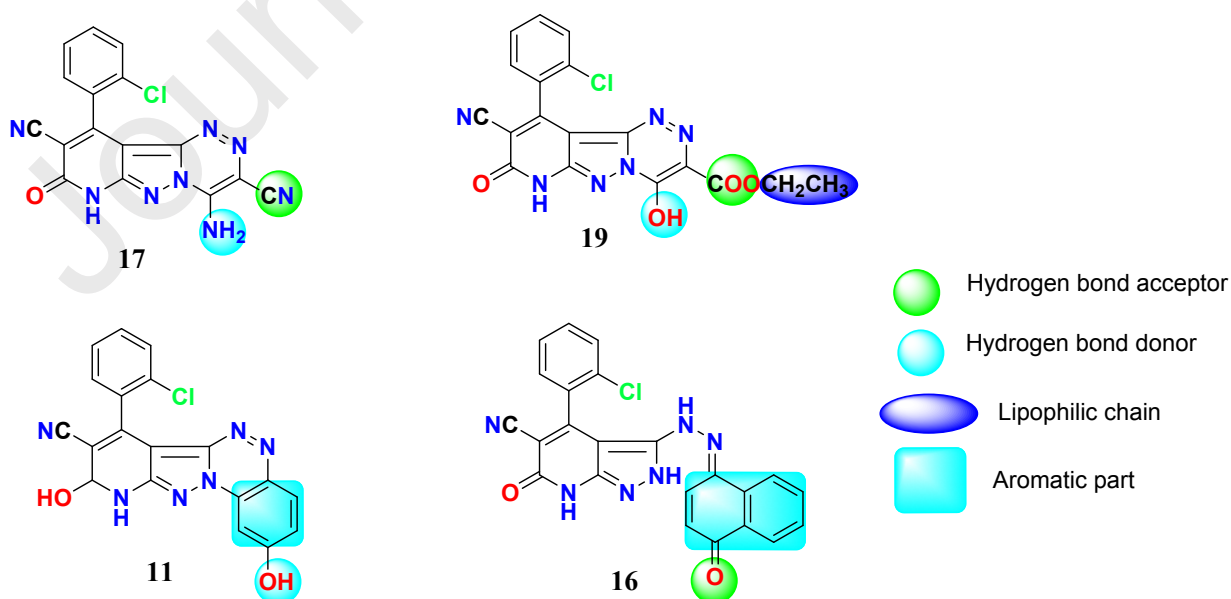


Fig. (2): Active compounds with highlighted pharmacophoric groups towards PIM-1 kinase

As shown in Fig (2), compounds with promising activities of both cytotoxic and PIM-1 kinase activities are represented to have active pharmacophoric groups, including hydrogen-bond acceptors or donors, lipophilic aliphatic or aromatic parts as incorporated to pyrazolo[3,4-b]pyridine as a common moiety. These promising activities may be due to the presence of these specific groups at these positions towards the PIM-1 kinase binding site, and hence towards the tested cytotoxic activity against MCF-7 cells.

2.2.3. Apoptotic investigation

Due to PIM-1 kinase overexpression in different types of cancers and their role in cancer progression pathways such as cell survival, cell cycle progression, and metastasis, so targeted Pim-1-kinase is an interesting approach to both apoptosis-induction and proliferation suppression by designing effective and selective inhibitors ²⁹. MCF-7 cancer cells were treated with compound **19** ($IC_{50} = 5.61 \mu\text{M}$, 48 h) and were investigated for their apoptosis-inducing activity using the cell cycle analysis with the cell population in different cell cycle phases.

2.2.3.1. Flow cytometric results

The study of the cell cycle is a crucial test showing the cell accumulation percentage in each growth phase with cytotoxic substances after treatment. As seen in Fig. (3), compound **19** significantly stimulated total apoptotic breast cancer cell death with 19.17-fold (31.25% compared to 1.63 for the control). Moreover, it slightly stimulated cell death *via* necrosis with 10.5-fold (11.03%, compared to 1.05% for the control). Furthermore, MCF-7 cancer cells after compound **19** treatment were subjected to DNA flow cytometry to analyze cell cycle kinetics study to assess the phase interaction of the compounds with the cell cycle. It increased G2/M cell (34.58%, compared to 12.26% for control) and pre-G1 (31.25%, compared to 1.64% for the control) population, and it decreased cell population in the G0/G1 (35.66% compared to 43.92% for control). Consequently, compound **19** induced pre-G1 and G2/M-phase cell cycle arrest and blocked the progression of MCF-7 cancer cells, which may be due to apoptosis induction of the tested compound by cell-cycle arrest at G2/M that deteriorate the genetic metrical. Our results are following previous studies ^{30,31}, which reported that the PIM-1 inhibition would have apoptosis-inducing activity through cell cycle arrest at G2/M phase transition. Additionally, it was reported by Bachmann et al. 2004 ³², who proved a novel function for Pim-1 in the G2/M cell cycle process as a positive regulator.

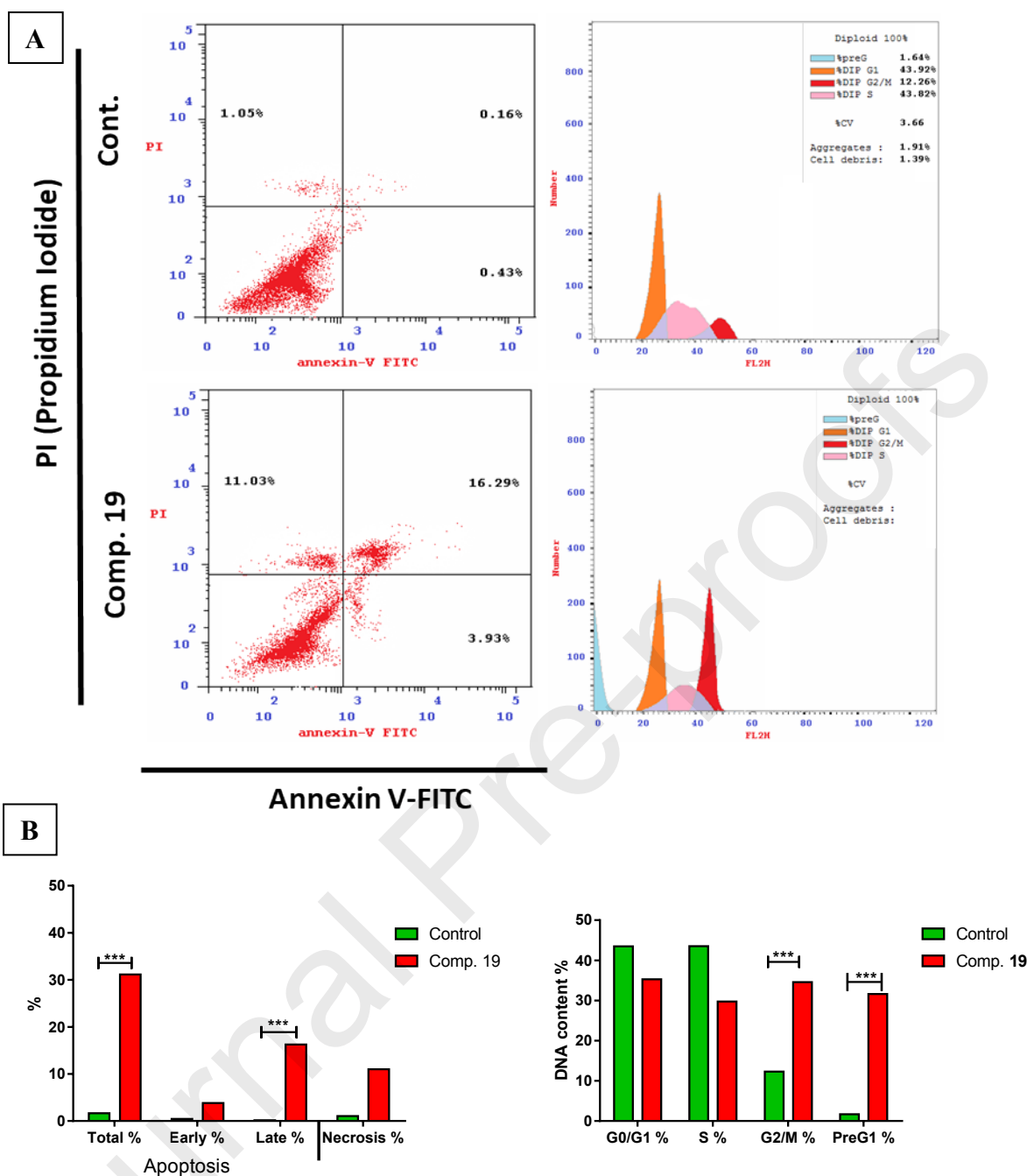


Fig. (3): A: FITC/Annexin-V-FITC/PI differential apoptosis/necrosis and DNA content-flow cytometry aided cell cycle analyses of both untreated and treated MCF-7 treated with compound **19** (IC_{50} = 5.61 μ M, 48 h). “Quadrant charts show Q2-1 (necrotic cells, AV-/PI+), Q2-2 (late apoptotic cells, AV-/PI+), Q2-3 (normal cells, AV-/PI-), Q2-4 (early apoptotic cells, AV+/PI-)”, **B:** Bar chart representation of the apoptosis percentages and the cell population percentage in various phases of the cell cycle.

2.2.3.2. Gene expression level (RT-PCR)

Based on the significant cytotoxic results and PIM-1 kinase inhibitory activity, compound **19** (IC_{50} = 5.61 μ M against MCF-7, IC_{50} = 26 nM against PIM-1) was thought worthwhile to be

further investigated for apoptosis induction in the **19**-treated MCF-7 cancer cells. As shown in Fig. (4), Compound **19** significantly activated the level of the P53 gene (with an increase of ≈ 4.2 -fold) with concomitant activation of the MDM2 level (with an increase of ≈ 3.9 -fold). It also increased the expression level of the pro-apoptotic PUMA gene (with an increase of ≈ 6.32 -fold). Accordingly, the compound activated cascade reaction of caspases 3, 9 activation with 7.90 and 6.56, respectively enhancing the proposed intrinsic apoptotic pathway.

Many tumor suppressive proteins such as p53, a key transcription factor in cell cycles arrested and DNA impaired cells, control PIM kinases. The p53 acts as an abnormal gene to allow different target gene expression that mediates p53 reactions. The p53 builds on in cells and is responsible in different stress conditions for DNA repair, cell cycle arrest, and apoptosis. The degradation of both p53 and MDM2 is disrupted by PIM kinase leading to increased p53 expression³³⁻³⁵, that's like we observed in our study results. On the other side, the anti-apoptotic Bcl-2 gene was considerably inhibited (decrease of ≈ 0.41 -fold). Meanwhile, it inhibited the PIM-1 kinase gene (decrease of ≈ 0.25 -fold). The results follow the PIM-1 inhibitory activity of compound **19** and with the proposed apoptotic pathway for its anti-cancer activity.

The pro-survival effect of PIM Kinase was demonstrated through Bcl-2 family gene control that regulates cell mortality by pro-apoptotic and anti-apoptotic proteins. Pro-apoptotic proteins include Poor and BAX, while anti-apoptotic proteins are Bcl-2 and Bcl-XL³⁶. Our results are following previous literature, in which it was reported that Pim-1 phosphorylation leads to BAD "Bcl-2 associated death promoter" phosphorylation and is chelated into p-BAD protein heterodimers that result in lower levels of free BAD that can bind the Bcl-2 "anti-apoptotic protein" and cause release of Bax "the pro-apoptotic protein"^{37,38}. As a result, Pim-1-kinase deficiency potentiates and eventually produces apoptosis pro-apoptotic proteins as previously reported by Aho et al. 2004³⁹.

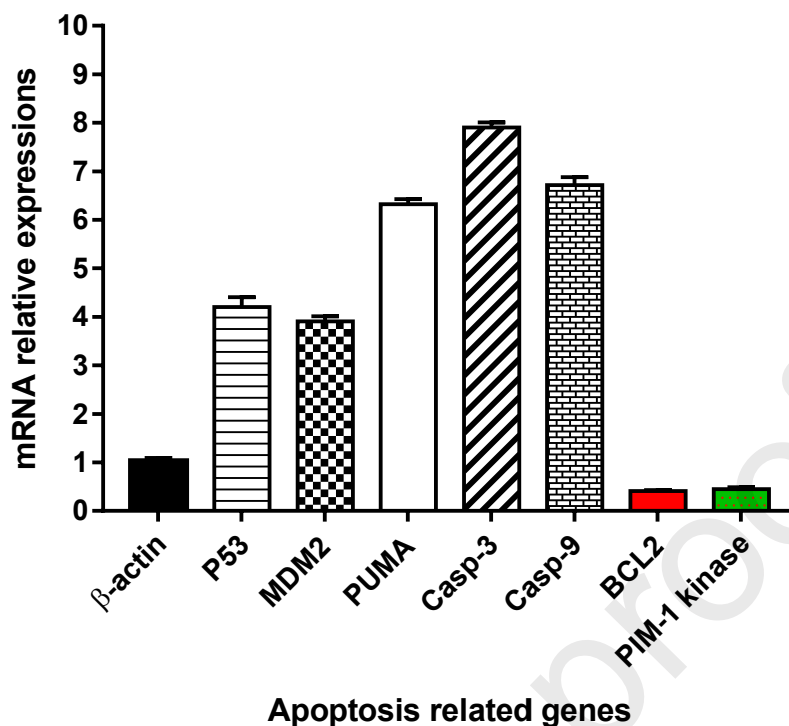


Fig. (4): mRNA gene expression of apoptosis-related genes was performed for MCF-7 cells were treated with Compound **19** ($IC_{50}=5.61 \mu\text{M}$) for 48 h. Values are represented by Mean \pm SEM (3 independent trials).

2.3. *In silico* studies

2.3.1. Molecular docking

A trial to investigate the virtual mechanism of binding of the most active compounds **17** and **19**, we used the structure-based drug design tool for docking these compounds inside the PIM-1 kinase active site (PDB: 2OBJ and 4K0Y) to validate the multi-targeted PIM-1 kinase inhibitory activity. The co-crystallized ligands of both proteins form one hydrogen bond with the Lys 67 as the interactive key amino acid, additionally with the lipophilic interactions. Docking results with analysis of ligand-receptor interactions, distances, and interactive moieties are summarized in Table (3) with 3D images.

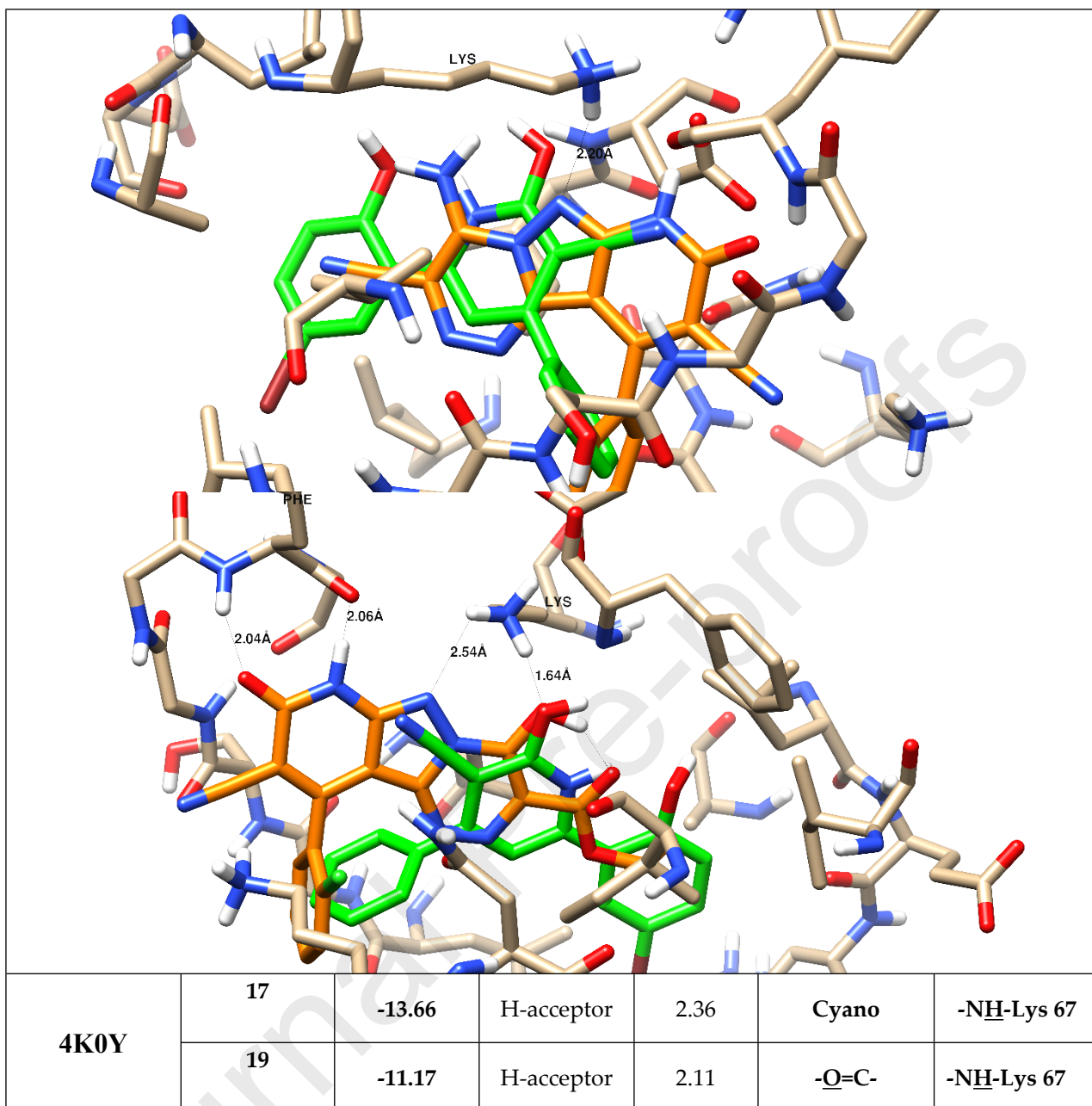
Regarding **2OBJ**, both compounds were docked inside the protein active sites with binding energies -15.22 and -13.37 Kcal/mol, respectively. Compound **17** forms one HB, while compound **19** forms two hydrogen bonds with Lys 67, as hydrogen bond acceptor in both compounds. Additionally, compound **19** forms two HB with Phe 49 amino acid one as HB donor and the other as HB acceptor, which is also an important amino acid for its inhibitor activity. Regarding **4K0Y**, both compounds were also docked inside the protein's pocket with binding energies -13.66 and -11.17 Kcal/mol, respectively. Both compounds form one HB as Hb acceptor with the interactive amino acid Lys67. Both compounds form lipophilic interactions with

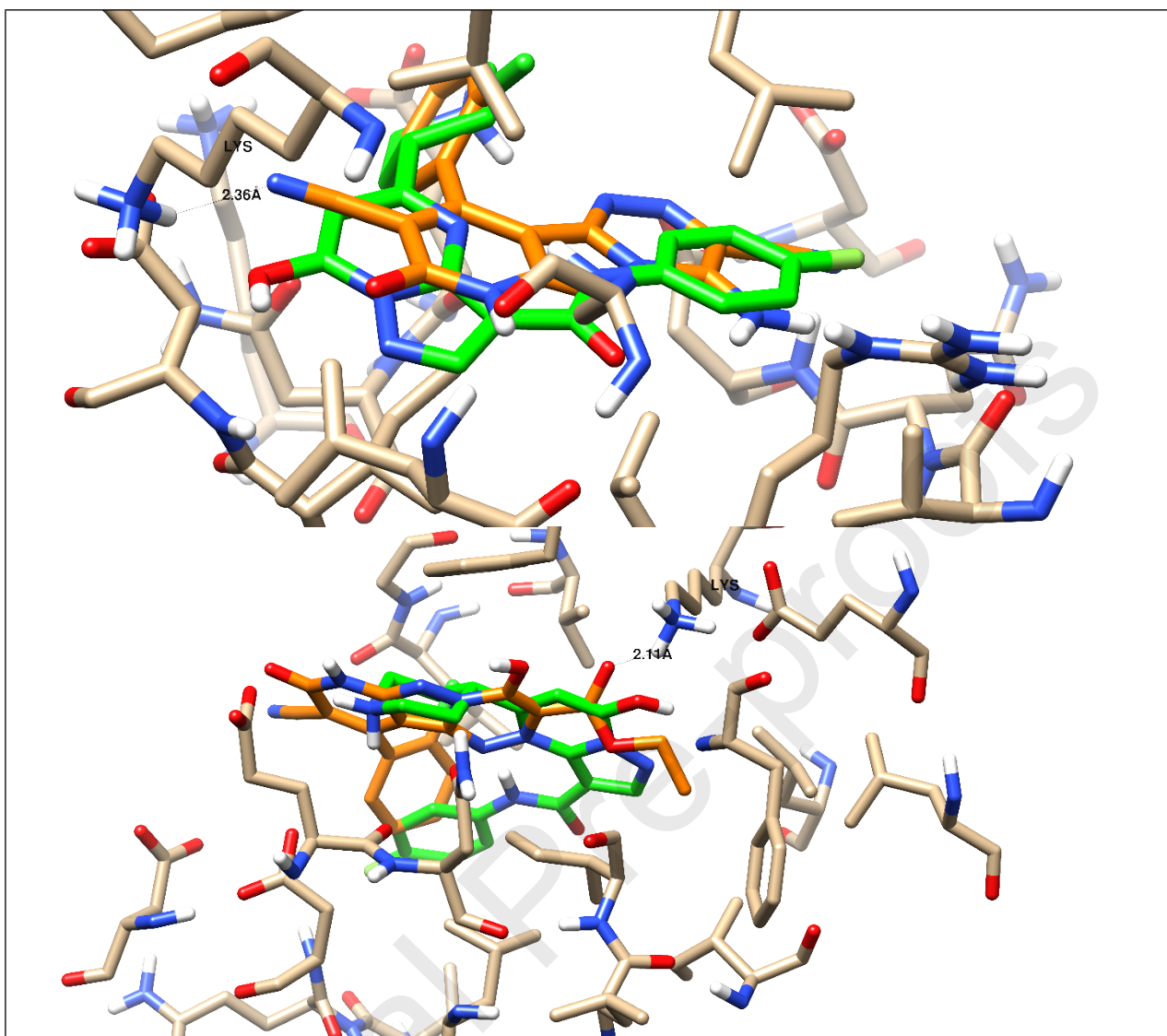
lipophilic amino acids inside the two proteins binding sites, which are; Val 52, Ala 65, Ile 104, Leu 120, leu 174, Ile 185, and Phe 49.

The docking studies with the two tested proteins indicated that both designed compounds showed promising binding activity as PIM-1 kinase inhibitors. This may be the proposed anti-breast cancer mode of action. This is because the docking results of both drug candidates 5 and 7 are following both RT-PCR and PIM-1 inhibitory kinase activity.

Table (3): Analysis of ligand-receptor interactions with binding energies of docked compounds 17 and 19 towards 2OBJ and 4K0Y (PIM-1 kinase)

| Protein (PDB code) | Docked compounds | Binding affinity (Kcal/mol) | Type on interaction | Bond length (Å) | Interaction moiety involved | Amino acid |
|--------------------|------------------|-----------------------------|---------------------|-----------------|-----------------------------|-------------|
| 2OBJ | 17 | -15.22 | H-acceptor | 2.20 | -N- | -NH-Lys 67 |
| | 19 | -13.37 | H-acceptor | 2.54 | -N- | -NH-Lys 67 |
| | | | H-acceptor | 1.64 | -OH- | -NH-Lys 67 |
| | | | H-donor | 2.06 | -NH- | -O=C-Phe 49 |
| | | | H-acceptor | 2.14 | -O=C- | -H-N-Phe 49 |





*Superimposed compound **17** & **19** (Orange), and the co-crystallized ligand (Green) of the two studied **2OBJ**, and **4k0Y** proteins

2.3.2. ADME pharmacokinetics

The predicted ADME pharmacokinetics parameters, along with the computed drug-likeness scores for the most five active compounds **11**, **12**, **16**, **17**, and **19** are shown in Table (4). All tested compounds possess accepted values of H-bond donors (2-3) and H-bond acceptors (3-8), which are following the right criteria for hydrogen-bonding capacity for good drug permeability [19]. When the H-bond donors exceed 5, and the H-bond acceptors reach 10, drugs will be poorly absorbed. All compounds have log P values ≤ 5 , so they had good membrane permeability. All Compounds, indeed, showed TPSA values within the acceptable range.

Additionally, solubility of more than 0.0001 mg/L requirements was found to be met. To indicate their good bioavailability by oral administration. So, it could, therefore, be considered as drugs applicants for oral absorption, all of which compounds were obeyed to Lipinsky 's five

rule. Furthermore, all compounds showed positive values for drug-likeness scores which indicated that all compounds should be considered as drug-like. In highlight, compound **19**, exhibited good drug-likeness score of 0.29, as shown in Fig. (5).

Table (4): *In silico* ADME pharmacokinetics properties

| # | Molinspiration 2018.10 | | | | | | MolSoft | | | |
|-----------|------------------------|----------------------|-----------------------|-------------|----------|-------------|----------|----------|-------------------|---------------------|
| | MWt (D) | MV (A ³) | PSA (A ²) | Log p | nrotb | nviolations | HBA | HBD | Solubility (mg/L) | Drug-likeness score |
| 11 | 390.79 | 308.57 | 119.37 | 2.55 | 1 | 0 | 6 | 3 | 18.87 | 0.30 |
| 12 | 390.79 | 308.57 | 119.37 | 2.55 | 1 | 0 | 6 | 3 | 18.87 | 0.30 |
| 16 | 440.85 | 357.27 | 126.80 | 4.45 | 3 | 0 | 5 | 3 | 8.76 | 0.05 |
| 17 | 362.74 | 278.85 | 149.56 | 1.97 | 1 | 0 | 6 | 3 | 173.83 | 0.07 |
| 19 | 410.78 | 320.05 | 146.28 | 2.72 | 4 | 0 | 8 | 2 | 120 | 0.29 |

“Mwt: Molecular Weight, MV: Molecular Volume, PAS: Polar Surface Area, Log p: Log P: Octanol-water partition coefficient, nrotb: number of rotatable bonds, nviolations: number of violations, HBA: Hydrogen Bond Acceptor, HBD: Hydrogen Bond Donor” [43].

Drug-likeness model score: 0.29

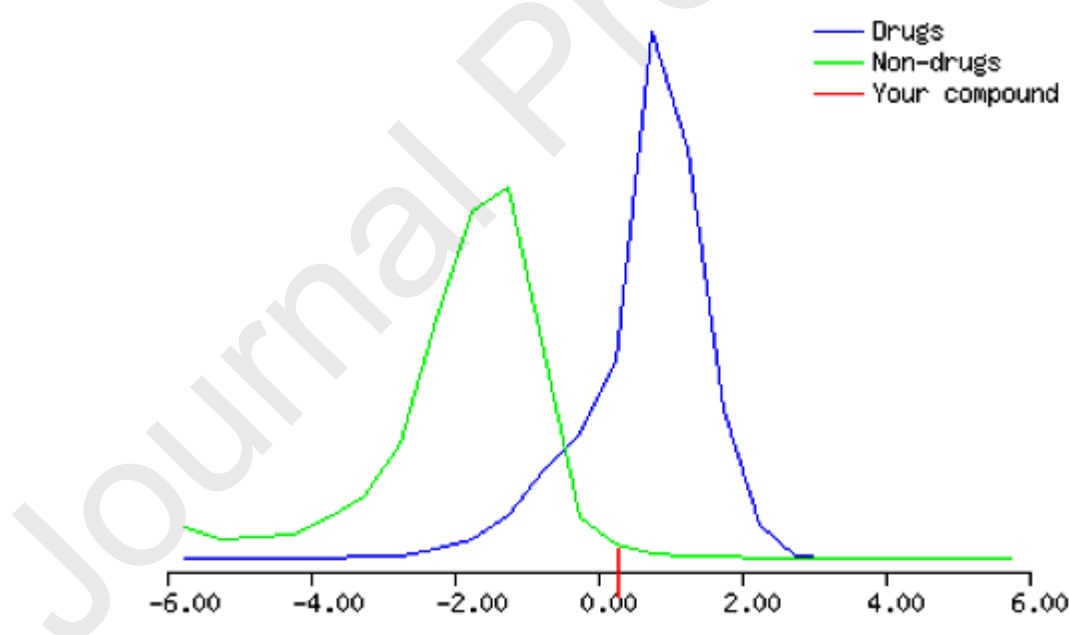


Fig. (5): Plot of Drug likeness score for the compound **19 (0.29)** using Molsoft. Blue-colored curve for drug like behavior, and green-colored curve for non-drug like behavior.

3. Experimental

3.1. Chemistry

All melting points are uncorrected; IR spectra (KBr): were recorded on pyeunicam SP-1000 cm⁻¹; ¹H-NMR and ¹³C-NMR spectra were recorded on a Burker DPX 200, spectrometer at 200 MHz (H¹) and 50 MHz (C¹³); chemical shifts (δ) are given relative to internal TMS at 295 K. For all new compounds satisfactory elemental analysis were obtained.

General synthesis for Preparation of 3,6-diaminopyrazolo[3,4-*b*]pyridine derivatives(3a-c):

A suspension of 2-amino-4-aryl-6-(thiophenyl)pyridine-3,5-dicarbonitrile **1a,1b** (10 mmol, 3.62g) in n-butanol (20 mL) was added (3 mL) hydrazine hydrate and methyl hydrazine was refluxed at 120-150 °C for two hour, and the precipitate was formed on hot, was filtered, dried and recrystallized from suitable solvent to give **3a-c** respectively.

3,6-Diamino-4-(2-chorophenyl)-1H-pyrazolo[3,4-*b*]pyridine-5-carbonitrile (3a): yellowish white crystals, 65% yield, m.p 280-282 °C. The ¹H-NMR in DMSO-*d*₆ δ 4.11 (s, 2H, NH₂ pyrazole), 6.80 (s, 2H, NH₂ pyridine) and 6.61-7.12 (m, 4H, Ar-H). Anal.calcd. For C₁₃H₉N₆Cl (284.7); C,54.84; H,3.19; N,29.52. Found: C,54.60; H,3.40; N,29.22. Compound was recrystallized from acetic acid.

3,6-Diamino-4-(3-chorophenyl)-1H-pyrazolo[3,4-*b*]pyridine-5-carbonitrile (3b): white crystals, yield (80%), m.p. 270-272 °C. The IR (KBr, cm⁻¹) at 3477, 3350, and 3311 (NH and NH₂), 2208 (cyano group) and 1624 (C=N group). The ¹H-NMR spectrum in DMSO-*d*₆ δ 4.31 (s, 2H, NH₂pyrazole), 6.79 (s, 2H, NH₂ pyridine), 7.41-7.62. (m, 4H, Ar-H). Anal.calcd. For C₁₃H₉N₆Cl (284.7); C,54.84; H,3.19; N,29.52. Found: C,54.50; H,3.35; N,29.22. Compound was recrystallized from ethanol.

3,6-Diamino-4-(2-chorophenyl)-1-methyl-pyrazolo[3,4-*b*]pyridine-5-carbonitrile(3c): golden yellow crystals, yield (82%), m.p 245-247 °C. The IR (KBr, cm⁻¹) at 3433, 3327 and 3216 (NH₂ group), 2926 (C-H aliphatic), 2198 (cyano group), 1648 (C=N group). The ¹H-NMR in DMSO-*d*₆ δ 3.54 (s, 2H, NH₂ pyrazole), 3.77 (s, 3H, CH₃), 5.44 (s, 2H, NH₂), 7.37-7.62 (m, 4H, Ar-H). The ¹H-NMR in CDCl₃ : δ 3.45 (br, 2H, NH₂), 3.70 (s, 3H, CH₃), 5.30 (s, 2H, NH₂ pyridine), 7.32 (d, J= 7.2Hz, 1H, H-aromatic), 7.40 (dd, J=15.2, 7.7 Hz, 2H, H-aromatic), 7.53 (d, J=7.7Hz, 1H, H-aromatic). The ¹³C-NMR in CDCl₃ 33.33 (CH₃), 86.93, 100.20, 116.85, 127.93, 130.58, 130.88, 131.42, 131.85, 132.73, 132.81, 147.58, 149.34, 150.77, 158.93 (Ar-C and cyano group). Anal.calcd. For C₁₄H₁₁N₆Cl (298.73); C,56.29; H,3.71; N,28.13. Found: C,56.75; H,3.90; N,28.10. Compound was recrystallized from acetic acid.

Synthesis of 4,4'-(1,4-phenylene)bis(2-amino-6-(phenylthio)pyridine-3,5-dicarbonitrile (6)

Method (A)

A mixture of terephthaldehyde **4** (1.34g, 0.01 mole), malononitrile (2.6g, 0.04 mole) and thiophenol (0.02 mole, 2.2g) were refluxed in ethanol (20 mL) and three drops of triethyl amine at 120-150 °C for 3 hours then the product formed was filtered, dried and recrystallized from ethanol to give **(6)**.

Method (B)

A mixture of compound **5** (2.32g, 0.01 mole), malononitrile (1.32g, 0.02mole) and thiophenol (2.2g, 0.02 mole) were refluxed in ethanol (20 mL) and three drops of triethyl amine at 120-150 °C for one hour then the product formed was filtered, dried and recrystallized from ethanol to give **(6)** Scheme 3.

4,4'-(1,4-phenylene)bis(2-amino-6-(phenylthio)pyridine-3,5-dicarbonitrile (6) : as yellow powder yield 55%, m.p. 340-342 °C. IR (KBr, cm⁻¹): 3451, 3329 and 3217(NH₂), 2209 (4C≡N), 1621 (C=N). ¹H NMR in (CDCl₃) δ ppm: 5.47(d, 4H, 2NH₂) and 7.10-7.68 (m, 14H, Ar-H). Also, The ¹H NMR in (DMSO-d₆) δ ppm: 6.00 (s, 2H, NH₂), 6.82 (s, 2H, NH₂) and 7.42-7.85 (m, 14H, Ar-H). M/S (m/z): 576 for [M⁺-2], 563 (M⁺-NH), 562 (M⁺-NH₂), 544 (M⁺-2NH₃), 501 (M⁺-H-ph), the base peak at 169 (100%) and aromatic fragmentation. Compound was recrystallized from ethanol.

General method for preparation of (7a, 7b) :

A mixture of **6** (0.001 mol, 0.578 g) was added (15 mL) of hydrazine hydrate and /or methyl hydrazine was heated under reflux at 150°C for four hours, left to cool at room temperature; The resulting product was filtered, dried, recrystallized from suitable solvent to give **7a** and **7b** respectively (Scheme 4) .

4,4'-(1,4-phenylene)bis(3,6-diamino-1H-pyrazolo[3,4-b]pyridine-5-carbonitrile) (7a): as yellow powder, Yield: 77% , m.p 300 °C; IR (KBr, cm⁻¹): 3460, 3302 and 3215 (NH and NH₂), 2205 (2 C≡N) and 1633 (C=N); ¹H-NMR in DMSO-d₆: δ 4.26 (br, 4H, 2NH₂ pyrazole), 6.85-6.95 (d, 4H, 2NH₂ pyridine), 7.33-7.78 (m, 4H, Ar-H) and 11.65 (br, 2H, 2NH pyrazole); MS (m/z): 421 (M⁺1). Anal. Calcd. For C₂₀H₁₄N₁₂ (422.406); C,56.87; H,3.34; N, 39.79 Found: C,56.55; H,3.04 ; N, 39.44. Compound was recrystallized from DMF.

4,4'-(1,4-phenylene)bis(3,6-diamino-1-methyl-1H-pyrazolo[3,4-b]pyridine-5-carbonitrile) (7b): yellow powder yield 64%, m.p. >300°C; ¹H-NMR in (DMSO-d₆): δ 3.62 (s, 6H, 2CH₃), 4.60 (br, 4H, 2NH₂pyrazole), 6.90 (s, 4H, 2NH₂ pyridine) and 11.85 (s, 4H, Ar-H). Anal. Calcd. For C₂₂H₁₈N₁₂ (450); C,58.66; H,4.03; N, 37.31.Found ; C,58.88 ; H,4.23; N, 37.55. Compound was recrystallized from chloroform.

Preparation of pyrido[2,3':3,4]pyrazolo[5,1-c][1,2,4]triazine derivatives :**General synthesis of compounds (11, 12, 14, 16):**

Diazonium salt **8a** was prepared from **3a** by diazotization with 30% sodium nitrite (0.02 mol, 1.38g) in presence of 63% Conc HNO₃ (15 mL) at 0-5 °C. A solution of resorcinol(1.2g, 10mmol), *p*-dihydroquinone (1.2g, 10 mmol), β -naphthol and/or α -naphthol (1.4g, 10 mmol) in ethanol (30 mL) was treated with a solution of sodium acetate trihydrate (5g) in water (12 mL). A solution of diazonium salt **8a** (0.01mol) was then added in small portions (during 10 min), followed with stirring for 2h. The hydrazone obtained was refluxed in acetic acid with stirring for 2h and the solid formed during boiling give **11, 12, 14, 16**, respectively.

7-(2-Chlorophenyl)-2-hydroxy-9-oxo-9,10-dihydrobenzo[e]pyrido[2,3':3,4]pyrazolo[5,1-c][1,2,4]triazine-8-carbonitrile (11): dark red powder, Yield (78%), m.p. 280-282 °C; IR (KBr, cm⁻¹) 3745 (OH), 3480 (NH), 2218 (C≡N), 1672 (C=O pyridone); ¹H-NMR in DMSO-*d*₆: δ 7.0-8.40 (m, 7H, Ar-H), 9.00 (s, 1H, OH) and 12.30 (br, 1H, NH pyridone). Anal.Calcd. For C₁₉H₉N₆ClO₂ (388.7); C,58.70; H,2.33; N,21.62. Found: C,58.50; H,2.16; N,21.32. Compound was recrystallized from DMF/H₂O.

7-(2-Chlorophenyl)-3-hydroxy-9-oxo-9,10-dihydrobenzo[e]pyrido[2,3':3,4]pyrazolo[5,1-c][1,2,4]triazine-8-carbonitrile (12): brownish yellow powder, Yield (67%), m.p.>300 °C; U.V 614, 500 and 402 nm . The IR (KBr, cm⁻¹), 3332 (OH), 3191 (NH), 2217 (C≡N), 1674 (C=O pyridine); ¹H-NMR in DMSO-*d*₆: δ 6.96-8.16 (m, 7H, Ar-H), 12.51 (br, 1H, OH) and 13.76 (br, 1H, NH pyridone). Anal.Calcd. For C₁₉H₉N₆ClO₂ (388.7); C,58.70; H,2.33; N,21.62. Found: C,58.46; H,2.12; N,21.33. Compound was recrystallized from DMF.

9-(2-Chlorophenyl)-11-oxo-11,12-dihydronaphtho[2,1-e]pyrido[2,3':3,4]pyrazolo[5,1-c][1,2,4]triazine-10-carbonitrile (14): reddish brown powder, Yield (82%), m.p. 300 °C; IR (KBr, cm⁻¹) 3438 (NH), 2218 (C≡N), 1668 (C=O pyridone) and 1612 (C=N). U.V in DMF: 618, 450, 370 and 336 nm.(conjugated and auxochrome system). ¹H-NMR in DMSO-*d*₆: δ 6.90 (d, 1H, Ar-H), 7.40-7.93 (m, 7H, Ar-H), 8.82 (d, 1H, Ar-H), 9.30 (d, 1H, Ar-H) and 13.50 (br, 1H, NH). Anal.Calcd. For C₂₃H₁₁N₆ClO (422.82); C,65.33; H,2.62; N,19.88. Found: C,65.60; H,2.80; N,19.51. Compound was recrystallized from DMF/H₂O.

(E)-4-(2-Chlorophenyl)-6-oxo-3-(2-(4-oxonaphthalen-1(4H)-ylidene)-6,7-dihydro-1H-pyrazolo[3,4-*b*] pyridine-5-carbonitrile (16): brown powder, Yield (60%), m.p.>300 °C. U.V in DMF 618, 444 and 334 nm ; IR(KBr, cm⁻¹); 3315 (OH), 3184 (NH), 2222 (C≡N), 2138 (conjugated azo compound), 1655 (C=O pyridone) and 1584 (C=C bond); ¹H-NMR in DMSO-

d_6 : δ 7.10-8.35 (m, 10H, Ar-H), 10.0 (br, 1H, OH) and 12.80 (br, 1H, NH pyridone); $^1\text{H-NMR}$ in CDCl_3 : δ 5.69 (s, 1H, OH pyridine), 7.40-8.08 (m, 9H, Ar-H), 8.45 (d, 1H, Ar-H), and 12.18 (s, 1H, OH). Anal Calcd. For $\text{C}_{23}\text{H}_{13}\text{N}_6\text{ClO}_2$ (440.8); C,62.66; H,2.97; N,19.06. Found: C,62.35; H,2.62; N,19.26. Compound was recrystallized from DMF.

General Synthesis of compounds (17-20):

A solution of an active hydrogen reagent (10 mmol, 0.66g) malononitrile, (10 mmol, 1.13g) ethyl cyanoacetate, (10 mmol, 1.6g) diethyl malonate and (10 mmol, 1.02g) acetyl acetone in ethanol (30 mL) was treated with a solution of sodium acetate trihydrate (5g) in water (10 mL). A solution of pyrazolo[3,4-*b*]pyridine diazonium nitrate **8a** (10mmol) in acetic acid was then added in small portions (10 min) with stirring. The reaction mixture was stirred at room temperature for three hours and the solid product obtained washed several times with cold water and dried to afford the corresponding hydrazone. The hydrazones were refluxed in acetic acid or ethanol solution containing (1 mL) of HCl for two hours and the precipitated solid was recrystallized from a suitable solvent to give compounds (17-20) respectively.

4-Amino-10-(2-chlorophenyl)-8-oxo-7,8-dihydropyrido[2,3':3,4]pyrazolo[5,1-*c*]-1,2,4-triazin-3,9-dicarbonitrile (17): Yield (64%), m.p 300-310 °C; U.V. in DMF 482, 460, 424, 386 and 344 nm ; IR (KBr, cm^{-1}) 3474 (OH), 3320 (NH_2), 2231 ($\text{C}\equiv\text{N}$), 1662 ($\text{C}=\text{O}$ pyridone) and 1611 ($\text{C}=\text{N}$ bond); $^1\text{H-NMR}$ in $\text{DMSO-}d_6$: δ 7.60-7.77 (m, 4H, Ar-H), 9.59 (br, 2H, NH_2) and 13.24 (br, 1H, NH). Anal.Calcd. For $\text{C}_{16}\text{H}_7\text{N}_8\text{ClO}$ (362.7); C,52.98; H,1.95; N,30.89. Found: C,52.65; H,1.69; N,30.66. Compound was recrystallized from AcOH.

10-(2-Chlorophenyl)-4,8-dihydroxyprido[2,3':3,4]pyrazolo[5,1-*c*]-1,2,4-triazine-3,9-dicarbonitrile (18): Yield (80%), m.p 240-242 °C; U.V. 484, 452, 390, 376 and 342 nm. IR (KBr, cm^{-1}) 3400 (OH), 3341 (NH), 2220, 2142 (2 $\text{C}\equiv\text{N}$), 1623 ($\text{C}=\text{N}$ bond) and 1558 ($\text{C}=\text{C}$ bond); $^1\text{H-NMR}$ in CDCl_3 at 5.78 (s, 2H, 2OH), and 7.41-7.55 (m, 4H, Ar-H). Anal.Calcd. For $\text{C}_{16}\text{H}_6\text{N}_7\text{ClO}_2$ (363.7); C,52.84; H,1.66; N,26.96. Found: C,52.60; H,1.40; N,26.70. Compound was recrystallized from ethanol.

Ethyl-10-(2-chlorophenyl)-9-cyano-4,8-dihydroxyprido[2,3':3,4]pyrazolo[5,1-*c*]-1,2,4-triazine-3-carboxylate (19): Yield (62%), m.p. 278-280 °C; IR (KBr, cm^{-1}), 3454 (OH), 3312 (NH), 2924 (C-H aliphatic bond), 2223 ($\text{C}\equiv\text{N}$), 2138 (conjugated cyano group), 1710 ($\text{C}=\text{O}$ ester), 1623 ($\text{C}=\text{N}$ bond) and 1552 ($\text{C}=\text{C}$ bond). Anal.Calcd. For $\text{C}_{18}\text{H}_{11}\text{N}_6\text{ClO}_4$ (410.7); C,52.63; H,2.70; N,20.46. Found: C,52.93; H,3.00; N,20.66. Compound was recrystallized from EtOH/DMF.

3-Acetyl-10-(2-chlorophenyl)-8-hydroxy-4-methylpyrido[2,3':3,4]pyrazolo[5,1-c]-1,2,4-triazine-8-carbonitrile (20): Yield (66%), m.p>300 °C; IR (KBr, cm⁻¹) 3339 (OH), 3213 (NH), 2219 (C≡N), 1685 (C=O) and 1617 (C=N bond) and 1558 (C=C bond); ¹H-NMR in CDCl₃: δ 2.04 (s, 3H, CH₃), 2.89 (s, 3H, COCH₃), 5.58 (br, 1H, OH) and 7.46 (m, 4H, Ar-H). Anal.Calcd. For C₁₈H₁₁N₆ClO₂(378.7); C,57.08; H,2.93; N,22.19. Found: C,57.28; H,3.10; N,22.30. Compound was recrystallized from EtOH / DMF.

Reaction of 7a with β-naphthol

A solution of compound 7a (0.01 mol ,4.62g) in 63% Conc. HNO₃ (6 mL) was diazotized with sodium nitrite (1.38g, 0.02) in water (4 mL) at 0-5 °C ; The cooled solution was added in small portion to a solution of β-naphthol (0.02 mol, 2.8g) and sodium acetate (6g) in 30 mL ethanol with stirring gave acyclic compound 21 and when heated in DMF in presence of 1 mL AcOH for one hour give cyclized compound 22.

9,9'-(1,4-phenylene)bis(11-aminonaphtho[2,1-e]pyrido[2',3':3,4]pyrazolo[5,1-c][1,2,4-triazine-10-carbonitrile (22): as brownish red Yield (77%), recrystallized from chloroform, m. p > 350 °C. ¹H-NMR in DMSO-*d*₆ : δ 6.60 (br, 4H, 2NH₂) and 7.00-9.00 (m, 16H, Ar-H). ms (m/e) 692 (M⁺-2), 346, 300 , 297, 234, 174, 130 and 88. Compound was recrystallized from EtOH/DMF.

3.2. Biology

3.2.1. Cytotoxic screening using MTT assay

Cytotoxic activity of all synthesized compounds against two breast cancer cell; MCF-7 (ERα-dependent), and MDA-MB-231 (Non-ERα-dependent), and non-cancerous breast cells; MCF-10A was determined by the MTT assay ⁴⁰. Cells were cultured according to standard protocols illustrated in ⁴¹. Serial concentrations of (0.1, 1, 10, 100, 1000) of tested compounds were prepared for treatment the cultured cells for 48h of incubation. After treatment, percentages of cell survival was determined by measuring the optical absorbance λ₅₇₀ nm according to the following equation; % of cell viability= $\frac{A_{sample}}{A_{control}} \times 100$, then IC₅₀ calculation was calculated using GaphPad prism 7 software ⁴².

3.2.2. PIM-1 kinase inhibitory activity

Top five active compounds were evaluated for their ability towards induction PIM-1 kinase inhibition using “HTScan® Pim-1 Kinase Assay Kit #7573”. They were dissolved in DMSO, and four serial concentrations were prepared following Abdelaziz et al 2018 ⁴³ and the manufacturer ‘instructions ⁴⁴.

3.2.3. Apoptosis investigation assays

3.2.3.1. Flow cytometric analysis

MCF-7 cancer cells were treated with compound **19** ($IC_{50} = 5.61 \mu\text{M}$, 48 h), compared to untreated cells as control, then flow cytometric analyses were carried to investigate the apoptotic mechanistic mode of action and were carried out as previously described by ⁴⁵. For the detailed methodology of flow cytometric analyses including FITC/Annexin-V-FITC/PI differential apoptosis/necrosis, DNA content-flow cytometry aided cell cycle (See supplementary).

3.2.3.2. Gene expression (RT-PCR) analysis

MCF-7 cancer cells were treated with compound **19** ($IC_{50} = 5.61 \mu\text{M}$, 48 h), then total RNA was extracted from cells using Qiagen's RNA extraction in both treated and untreated. The synthesis of cDNA was then performed, followed by the qPCR test in one tube. The perfect primer pairs (**Supplementary, Table 1**) were selected for the tested genes (P53, MDM2, PUMA, CASP-3, -9, PIM-1, BCL2) and β -actin as a housekeeping gene. The results were given in cycle thresholds (Ct), and $\Delta\Delta$ Ct for calculating the relative quantities of each gene tested as previously described by ⁴⁵⁻⁴⁷.

3.3. *In silico* studies

3.3.1. Molecular docking

The molecular docking towards the Pim-1 kinase active site was performed to demonstrate possible interactions. All synthesized derivatives were chemically and energetically optimized, and subject docking inside the PDB related codes of PIM-1 kinase (PDB=2OBJ and 4K0Y), their structures were also manipulated according to Nafie *et al.* 2019 ⁴⁸. MOE 2014 was used as the validated molecular docking calculation, and Chimera software was finally used as the visualized software for the analysis of docked compounds and protein interactions.

3.3.2. ADME pharmacokinetics

In silico ADME pharmacokinetics parameters of the most active compounds were calculated using a set of software including “MolSoft”, “Molinspiration”, and “SwissADME” websites as previously described by Youssef *et al.*, 2020 ^{49,50}.

4. Conclusion

Designing selective novel pyrazolo[3,4-*b*]pyridine PIM-1 kinase inhibitors as a promising approach for suppressing tumor proliferation via apoptosis induction level. So, a simple method for the preparation of 3,6-diaminopyrazolo[3,4-*b*]pyridine derivatives **3a-c** from 2-amino-6-thiophenylpyridine-3,5-dicarbonitrile derivatives **1a,b** was described. In the same

way, the reaction of 2-amino-4-(4-(2-amino-3,5-dicyano-6-thiophenylpyridin-4-yl) phenyl)-6-thiophenylpyridine-3,5-dicarbonitrile **6** with hydrazin hydrate or methyl hydrazine give **7a** and **7b** respectively, via thiophenol elimination and cyclization. Reaction of the diazonium salt **8a** with resorcinol, *p*-dihydroquinone, β -naphthol and/or α -naphthol yield pyrido[3',2':4,5]pyrazolo[3,2-*c*]1,2,4-triazine **11**, **12**, **14** and **16** respectively. The reaction of diazonium salt **8a** with appropriate active hydrogen reagents namely malononitrile, ethyl cyanoacetate, diethylmalonate and acetyl acetone, give **17-20** in good yield. Finally, treatment diazonium salt of compound **7a** with β -naphthol afforded compound **22** in good yield. Chemical and spectroscopic evidence is provided for new compound structures. All the synthesized derivatives were screened for their activity and selectivity against two breast cancer cell lines and one normal breast cancer cells. Some of them exhibited potent cytotoxic activity especially, **17** and **19** with IC₅₀ values 6.98 and 5.61 μ M against MCF-7 cells, aligned with potent PIM-1 inhibitory kinase activity with IC₅₀ values 43 and 26 nM, respectively compared to the reference drug with IC₅₀ value 17 nM. Induction of apoptosis of compound **19** was investigated through activating pro-apoptotic genes P53, MDM2, Bax with activating caspases 3,9 and inhibiting anti-apoptotic genes BCL2 and PIM-1 kinase. Finally, the PIM-1 inhibition activities for compounds **17** and **19** were following the molecular docking study that revealed good binding affinity towards the Pim-1 kinase active site.

Conflict of interest

The authors declare no conflict of interest. This research did not receive any specific grant from funding agencies in the public, commercial, or not-for-profit sectors

Electronic supporting information

The spectroscopic characterization charts of the investigated compounds together with detailed methodologies are provided as electronic supporting information at

Author's contribution

Eman S. Tantawy, **Anaiat K. Mohamed**, and **Atef M. Amer** synthesized the entire series of derivatives with characterization of structure elucidation, while **Mohamed S. Nafie** initiated the idea and design of the biology part by carrying out *in vitro* cytotoxic screening, flow cytometry, RT-PCR analysis, and *in silico* molecular docking. All authors contributed to data analysis and manuscript writing in their corresponding parts. **Mohamed S. Nafie** carried out the linguistic revision for the whole manuscript and validated it in the final submitted form, additionally, he followed up the publication process from submission through the review to acceptance.

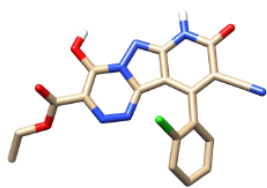
References

1. Torre LA, Islami F, Siegel RL, et al. Global Cancer in Women: Burden and Trends. *Cancer Epidemiol Biomarkers Prev.* 2017;26:444–457.
2. Malinen M, Jääskeläinen T, Pelkonen M, et al. Proto-oncogene PIM-1 is a novel estrogen receptor target associating with high grade breast tumors. *Mol. Cell. Endocrinol.* 2013;365:270–276.
3. Asati V, Mahapatra DK, Bharti SK. PIM kinase inhibitors: Structural and pharmacological perspectives. *Eur. J. Med. Chem.* 2019;172:95–108.
4. Santio NM, Koskinen PJ. PIM kinases: From survival factors to regulators of cell motility. *Int. J. Biochem. Cell Biol.* 2017;93:74–85.
5. Tursynbay Y, Zhang J, Li Z, et al. Pim-1 kinase as cancer drug target: An update. *Biomed Rep.* 2016;4:140–146.
6. Saris CJ, Domen J, Berns A. The pim-1 oncogene encodes two related protein-serine/threonine kinases by alternative initiation at AUG and CUG. *The EMBO Journal* 1991;10:655–664.
7. Wang Z, Bhattacharya N, Weaver M, et al. Pim-1: A serine/threonine kinase with a role in cell survival, proliferation, differentiation and tumorigenesis. *J. Vet. Sci.* 2001;2:167–179.
8. Panchal NK, Sabina EP. A serine/threonine protein PIM kinase as a biomarker of cancer and a target for anti-tumor therapy. *Life Sciences* 2020;255:117866.
9. Morwick T. Pim kinase inhibitors: a survey of the patent literature. *Expert Opin. Ther. Pat.* 2010;20:193–212.
10. Anizon F, Shtil AA, Moreau VND and P. Fighting Tumor Cell Survival: Advances in the Design and Evaluation of Pim Inhibitors. *Curr Med Chem.* 2010;17:4114–4133.
11. Malone T, Schäfer L, Simon N, et al. Current perspectives on targeting PIM kinases to overcome mechanisms of drug resistance and immune evasion in cancer. *Pharmacol. Ther.* 2020;207:107454.
12. El-Borai MA, Rizk HF, Beltagy DM, et al. Microwave-assisted synthesis of some new pyrazolopyridines and their antioxidant, anti-tumor and antimicrobial activities. *Eur. J. Med. Chem.* 2013;66:415–422.
13. Salem MS, Ali MAM. Novel Pyrazolo[3,4-*b*]pyridine Derivatives: Synthesis, Characterization, Antimicrobial and Antiproliferative Profile. *Biol. Pharm. Bull* 2016;39:473–483.
14. Chavva K, Pillalamarri S, Banda V, et al. Synthesis and biological evaluation of novel alkyl amide functionalized trifluoromethyl substituted pyrazolo[3,4-*b*]pyridine derivatives as potential anti-cancer agents. *Bioorg Med Chem Lett.* 2013;23:5893–5895.
15. Eissa IH, El-Naggar AM, El-Hashash MA. Design, synthesis, molecular modeling and biological evaluation of novel 1H-pyrazolo[3,4-*b*]pyridine derivatives as potential anti-cancer agents. *Bioorg. Chem.* 2016;67:43–56.

16. Mohamed MS, Awad YEE-D, El-Hallouty SM, et al. Design, Synthesis and Cancer Cell Line Activities of Pyrazolo[3,4-b]pyridine Derivatives. *OJMC* 2012;2:78–88.
17. Mohamed NR, Khaireldin NY, Fahmy AF, et al. Facile synthesis of fused nitrogen containing heterocycles as anti-cancer agents. *Der Pharma Chemica* 2010;2:400–417.
18. Metwally NH, Deeb EA. Synthesis, anti-cancer assessment on human breast, liver and colon carcinoma cell lines and molecular modeling study using novel pyrazolo[4,3-c]pyridine derivatives. *Bioorg. Chem.* 2018;77:203–214.
19. Sindhu J, Singh H, Khurana JM, et al. Synthesis and biological evaluation of some functionalized 1H-1,2,3-triazole tethered pyrazolo[3,4-b]pyridin-6(7H)-ones as antimicrobial and apoptosis inducing agents. *Med Chem Res* 2016;25:1813–1830.
20. Cheney IW, Yan S, Appleby T, et al. Identification and structure–activity relationships of substituted pyridones as inhibitors of Pim-1 kinase. *Bioorg Med Chem Lett.* 2007;17:1679–1683.
21. El-Gohary NS, Hawas SS, Gabr MT, et al. New series of fused pyrazolopyridines: Synthesis, molecular modeling, antimicrobial, anti-quorum-sensing and anti-tumor activities. *Bioorg. Chem.* 2019;92:103109.
22. El-Gohary NS, Shaaban MI. New pyrazolopyridine analogs: Synthesis, antimicrobial, anti-quorum-sensing and anti-tumor screening. *Eur. J. Med. Chem.* 2018;152:126–136.
23. El-Gohary NS, Shaaban MI. Design, synthesis, antimicrobial, anti-quorum-sensing and anti-tumor evaluation of new series of pyrazolopyridine derivatives. *Eur. J. Med. Chem.* 2018;157:729–742.
24. Chioua M, Samadi A, Soriano E, et al. Synthesis and biological evaluation of 3,6-diamino-1H-pyrazolo[3,4-b]pyridine derivatives as protein kinase inhibitors. *Bioorg Med Chem Lett.* 2009;19:4566–4569.
25. Chioua M, Soriano E, Samadi A, et al. Studies on the acetylation of 3,6-diamino-1H-pyrazolo[3,4-b]pyridine-5-carbonitrile derivatives. *J. Heterocycl. Chem.* 2010;47:861–872.
26. Abouzid KAM, Al-Ansary GH, El-Naggar AM. Eco-friendly synthesis of novel cyanopyridine derivatives and their anti-cancer and PIM-1 kinase inhibitory activities. *Eur. J. Med. Chem.* 2017;134:357–365.
27. Wenglowy S. Pyrazolo[3,4-b]pyridine kinase inhibitors: a patent review (2008 – present). *Expert Opin. Ther. Pat.* 2013;23:281–298.
28. Abdelaziz ME, El-Miligy MMM, Fahmy SM, et al. Design, synthesis and docking study of pyridine and thieno[2,3-b]pyridine derivatives as anti-cancer PIM-1 kinase inhibitors. *Bioorg. Chem.* 2018;80:674–692.
29. Chen WW, Chan DC, Donald C, et al. Pim family kinases enhance tumor growth of prostate cancer cells. *Mol Cancer Res* 2005;3:443–451.
30. Zhang X, Song M, Kundu JK, et al. PIM Kinase as an Executional Target in Cancer. *J Cancer Prev* 2018;23:109–116.

31. Bachmann M, Kosan C, Xing PX, et al. The oncogenic serine/threonine kinase Pim-1 directly phosphorylates and activates the G2/M specific phosphatase Cdc25C. *The Int. J. Biochem. Cell Biol.* 2006;38:430–443.
32. Bachmann M, Hennemann H, Xing PX, et al. The Oncogenic Serine/Threonine Kinase Pim-1 Phosphorylates and Inhibits the Activity of Cdc25C-associated Kinase 1 (C-TAK1) A NOVEL ROLE FOR Pim-1 AT THE G2/M CELL CYCLE CHECKPOINT. *J Biol Chem.* 2004;279:48319–48328.
33. Cen B, Mahajan S, Zemskova M, et al. Regulation of Skp2 Levels by the Pim-1 Protein Kinase. *J Biol Chem.* 2010;285:29128–29137.
34. Zhou BP, Liao Y, Xia W, et al. Cytoplasmic localization of p21Cip1/WAF1 by Akt-induced phosphorylation in HER-2/neu-overexpressing cells. *Nat Cell Biol.* 2001;3:245–252.
35. Zhou BP, Liao Y, Xia W, et al. HER-2/neu induces p53 ubiquitination via Akt-mediated MDM2 phosphorylation. *Nat Cell Biol.* 2001;3:973–982.
36. Asati V, Mahapatra DK, Bharti SK. PIM kinase inhibitors: Structural and pharmacological perspectives. *Eur. J. Med. Chem.* 2019;172:95–108.
37. Wendel H-G, De Stanchina E, Fridman JS, et al. Survival signalling by Akt and eIF4E in oncogenesis and cancer therapy. *Nature* 2004;428:332–337.
38. van Lohuizen M, Verbeek S, Krimpenfort P, et al. Predisposition to lymphomagenesis in pim-1 transgenic mice: cooperation with c-myc and N-myc in murine leukemia virus-induced tumors. *Cell* 1989;56:673–682.
39. Aho TLT, Sandholm J, Peltola KJ, et al. Pim-1 kinase promotes inactivation of the pro-apoptotic Bad protein by phosphorylating it on the Ser112 gatekeeper site. *FEBS Letters* 2004;571:43–49.
40. Mosmann T. Rapid colorimetric assay for cellular growth and survival: Application to proliferation and cytotoxicity assays. *J. Immunol. Methods.* 1983;65:55–63.
41. Freshney R.I., Culture of tumor cells, Culture of Animal Cells, John Wiley & Sons, Inc., 2010, pp. 463–479, , <https://doi.org/10.1002/9780470649367.ch24>.
42. Tantawy ES, Amer AM, Mohamed EK, et al. Synthesis, characterization of some pyrazine derivatives as anti-cancer agents: In vitro and in Silico approaches. *J. Mol. Struct.* 2020;1210:128013.
43. Abdelaziz ME, El-Miligy MMM, Fahmy SM, et al. Design, synthesis and docking study of pyridine and thieno[2,3-b] pyridine derivatives as anti-cancer PIM-1 kinase inhibitors. *Bioorg. Chem.* 2018;80:674–692.
44. CST - HTScan® Pim-1 Kinase Assay Kit Available from: www.cellsignal.com/products/cellular-assay-kits/htscan-pim-1-kinase-assay-kit/7573.
45. Nafie MS, Arafa K, Sedky NK, et al. Triaryl dicationic DNA minor-groove binders with antioxidant activity display cytotoxicity and induce apoptosis in breast cancer. *Chem.-Biol. Interact.* 2020;324:109087.

46. Kattan SW, Nafie MS, Elmgeed GA, et al. Molecular docking, anti-proliferative activity and induction of apoptosis in human liver cancer cells treated with androstane derivatives: Implication of PI3K/AKT/mTOR pathway. *J. Steroid Biochem. Mol. Biol.* 2020;198:105604.
47. Sarhan AAM, Boraei ATA, Barakat A, et al. Discovery of hydrazide-based pyridazino[4,5-*b*]indole scaffold as a new phosphoinositide 3-kinase (PI3K) inhibitor for breast cancer therapy. *RSC Adv.* 2020;10:19534–19541.
48. Nafie MS, Tantawy MA, Elmgeed GA. Screening of different drug design tools to predict the mode of action of steroidal derivatives as anti-cancer agents. *Steroids* 2019;152:108485.
49. Youssef E, El-Moneim MA, Fathalla W, et al. Design, synthesis and anti-proliferative activity of new amine, amino acid and dipeptide-coupled benzamides as potential sigma-1 receptor. *J IRAN CHEM SOC* . Epub ahead of print May 9, 2020. DOI: 10.1007/s13738-020-01947-6.
50. Gad EM, Nafie MS, Eltamany EH, et al. Discovery of New Apoptosis-Inducing Agents for Breast Cancer Based on Ethyl 2-Amino-4,5,6,7-Tetra Hydrobenzo[*b*]Thiophene-3-Carboxylate: Synthesis, In Vitro, and In Vivo Activity Evaluation. *Molecules* 2020;25:2523.

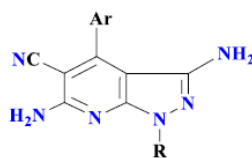


Compound 19, effective and selective with IC₅₀= 5.61 μM against MCF-7

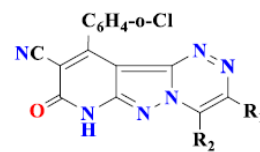


Synthesis of pyrazolo[3,4-b]pyridine

Novel pyrazolo[3,4-b]pyridine scaffold-based derivatives



3(a-c)



11-20

Apoptosis-inducing activity

- Apoptosis-inducing at G₂/M cell cycle arrest

PIM-1 inhibitory activity



- Superimposed binding mode as dual targeted PIM-1 kinase (PDB 2OBJ and 4K0Y) *in silico*
- Potent PIM-1 inhibitor activity 26 nM *in vitro*

Declaration of interests

The authors declare that they have no known competing financial interests or personal relationships that could have appeared to influence the work reported in this paper.

The authors declare the following financial interests/personal relationships which may be considered as potential competing interests:

Journal Pre-proofs